Numerical analysis of a baryon and its dilatation modes in holographic QCD

Keiichiro Hori and Hideo Suganuma
Department of Physics, Kyoto University, Kitashirakawaoiwake, Sakyo, Kyoto 606-8502, Japan

Hiroki Kanda
Yukawa Institute for Theoretical Physics (YITP), Kyoto University, Kitashirakawaoiwake, Sakyo, Kyoto 606-8502, Japan

(Received 31 July 2023; accepted 2 January 2024; published 24 January 2024)

We investigate a baryon and its dilatation modes in holographic QCD based on the Sakai-Sugimoto model, which is expressed as a $1+4$ dimensional $\mathrm{U}(N_f)$ gauge theory in the flavor space. For spatially rotational symmetric systems, we apply a generalized version of the Witten Ansatz, and reduce $1+4$ dimensional holographic QCD into a $1+2$ dimensional Abelian Higgs theory in a curved space. In the reduced theory, the holographic baryon is described as a two-dimensional topological object of an Abrikosov vortex. We numerically calculate the baryon solution of holographic QCD using a fine and large lattice with spacing of 0.04 fm and size of 10 fm. Using the relation between the baryon size and the zero-point location of the Higgs field in the description with the Witten Ansatz, we investigate a various-size baryon through this vortex description. As time-dependent size-oscillation modes (dilatation modes) of a baryon, we numerically obtain the lowest excitation energy of 577 MeV and deduce the dilatational excitation of a nucleon to be the Roper resonance $\mathrm{N}^*(1440)$.

DOI: 10.1103/PhysRevD.109.014030

I. INTRODUCTION

Quantum chromodynamics (QCD) is established as the fundamental theory of strong interaction and characterized by $\mathrm{SU}(N_c)$ gauge symmetry and global $\mathrm{SU}(N_f)_L \times \mathrm{SU}(N_f)_R$ chiral symmetry. Owing to asymptotic freedom of QCD, high-energy hadron reactions can be analyzed using perturbative QCD. In low energy regions, however, the QCD coupling becomes strong, and the perturbative method is no more applicable. Therefore, for theoretical analyses of hadrons based on QCD, some nonperturbative methods are necessary such as lattice QCD. Based on gauge/gravity duality [1] for D branes [2] in superstring theory, holographic QCD is an interesting new tool to analyze the nonperturbative properties of QCD [3–5].

Around 1970, the string theory was originally proposed by Nambu, Goto, and Polyakov for the description of hadrons [6–8]. After establishment of QCD, the string theory was not used for the main research of hadrons. Instead, this framework was reformulated as the superstring theory in the 1980s [9] and has been studied as a plausible candidate of a grand unified theory including quantum gravity, and many studies have been constantly conducted to date.

The superstring theory is formulated in 10 dimensional space-time and includes D branes, on which open string endpoints exist [2]. As a remarkable discovery by Polchinski, on the surface of N overlapped D branes, $\mathrm{U}(N)$ gauge symmetry emerges, and the N D-branes system leads to $\mathrm{U}(N)$ gauge theory [2]. In fact, on the N D-branes, gauge fields A_{ab} appear from the open string linking two D-branes labeled with a and b $(a, b = 1, 2, \ldots, N)$. On the other hand, around the D brane, a higher-dimensional supergravity theory is formed since the brane has mass, and multiple branes can be gravitational sources. Thus, there are two different theories relating to the D-brane, and the gauge theory *on* the D-brane and the higher-dimensional gravity theory *around* the D-brane are conjectured to be equivalent [1], which is called AdS/CFT correspondence or gauge/gravity duality. This remarkable equivalence between gauge and gravity theories was first proposed by Maldacena from a detailed analysis of four-dimensional $\mathcal{N}=4$ supersymmetric (SUSY) $\mathrm{SU}(N)$ Yang-Mills theory and five-dimensional anti–de Sitter (AdS) supergravity theory [1], using large N argument. This equivalence was first called as AdS/CFT correspondence and is generalized as gauge/gravity duality in more general concept. In this correspondence, a strong-coupling gauge theory can be described with a weak-coupling gravity theory [1,3–5].

With this correspondence, many researches have been performed, and one of the main category is to analyze strong-coupling QCD with a higher-dimensional classical gravity theory, which is called holographic QCD [3–5,10,11]. In 1998, Witten formulated a non-SUSY version of holographic QCD for a four-dimensional pure-gluon Yang-Mills theory using S^1-compactified N_c D4 branes, where periodic and antiperiodic boundary conditions are imposed on boson and fermion fields, respectively [3]. In 2005, Sakai and Sugimoto proposed holographic QCD for four-dimensional full QCD, including massless chiral quarks, by adding the N_f pair of D8 and $\overline{\mathrm{D8}}$ branes to S^1-compactified D4 branes [5]. In fact, the D4/D8/$\overline{\mathrm{D8}}$ multi-D-brane system has $\mathrm{SU}(N_c)$ gauge symmetry and $\mathrm{SU}(N_f)_L \times \mathrm{SU}(N_f)_R$ chiral symmetry and leads to massless QCD in infrared scale. Here, quarks and gluons appear from the massless modes of 4-8 and 4-4 strings, respectively. In the large N_c limit, N_c D4 branes are dominant as a gravity source and are converted into a gravitational field via the AdS/CFT correspondence or the gauge/gravity duality. The 't Hooft coupling $\lambda \equiv N_c g^2$ is a control parameter of the gauge side, and strong-coupling QCD with a large λ corresponds to a weakly interacting gravitational theory. Then, this system is described by the D8 brane in the presence of a background gravitational field originating from the D4 brane. Nonperturbative properties of QCD can be analyzed with a classical gravity theory.

In the leading order of $1/N_c$ expansion, the effective theory of the D8 brane in the D4-brane-induced background gravity is expressed with the Dirac-Born-Infeld (DBI) action and the Chern-Simons (CS) term. The leading order of $1/\lambda$ expansion is the DBI action, and the next leading of $1/\lambda$ is the CS term. Expanding the DBI action with $1/\lambda$, the leading order becomes a five-dimensional Yang-Mills theory in flavor space in a curved space, where a background gravity appears only in the fifth dimension. The CS term is a topological term responsible for anomalies in QCD. In holographic QCD, the five-dimensional holographic field is decomposed into four-dimensional meson fields, and this theory is successful in the mesons sector, that is, it describes low-lying meson masses, intermeson couplings, and phenomenological laws in hadron physics [5]. Regarding baryonic degrees of freedom, baryons do not appear explicitly in the holographic action. In fact, the baryon does not appear as a system component in holographic QCD.

The absence of baryons in the effective action is a general result due to the large N_c argument, because QCD is reduced into a weak-coupling theory of mesons and glueballs in the large N_c limit [12], where the baryon mass increases as $\mathcal{O}(N_c)$ and the baryon do not appear in the effective action. In the large N_c argument, the baryon is considered to appear as a soliton of mesons such as the Skyrmion in the Skyrme model [12–14].

Here, we briefly mention a historical overview of the Skyrme model. The Skyrme model is a low-energy effective theory in hadron physics, first proposed by Skyrme in 1961 [13]. After the quark model was proposed in 1964 [15], main researches of strong interaction and hadrons were shifted to the quark theory, which was eventually developed into QCD. In 1979, Witten revived the Skyrme soliton picture of baryons from a large N_c viewpoint of QCD [12], although the direct relation between the Skyrme model and QCD has not been clear. In 2005, Sakai and Sugimoto showed a theoretical explicit connection between massless QCD and the Skyrme Lagrangian, which is derived as the pion sector in holographic QCD, using the gauge/gravity duality for a D-brane system [5]. (Actually, the Sakai-Sugimoto model reduces into the Skyrme model, when massive mesons are dropped off, leaving only light pions.)

Now, let us concentrate on baryons in holographic QCD. Also for holographic QCD, which is derived with large N_c and is described with only meson fields, the baryon is described as a chiral soliton of mesons, that is, a topological object like a brane-induces Skyrmion [16,17] or an instantonlike object [18,19]. In fact, the baryon appears as an spatially extended object in holographic QCD.

To summarizes the above, holographic QCD is an analytical nonperturbative method for QCD and has direct connection with QCD, as a clearly strong advanced point. In holographic QCD, while mesons appear in the action and can be directly treated, the baryon is described as an extended soliton of mesons. Therefore, compared with the meson sector, the baryon sector is more difficult and has not been well studied in holographic QCD, in spite of several pioneering studies on the holographic baryon [16,19–24]. In addition, this baryonic soliton allows spatial dilatation modes as its excitation peculiar to the spatially-extended object, and thus we focus on this dilatation mode of the holographic baryon in the latter of our study.

In this study, we investigate a single baryon and its dilatation modes in holographic QCD, adopting the Sakai-Sugimoto model formulated as a $1+4$ dimensional $\mathrm{U}(N_f)$ gauge theory in the flavor space. For spatially rotational symmetric systems, we apply a generalized Witten Ansatz and reduce $1+4$ dimensional holographic QCD into a $1+2$ dimensional Abelian Higgs theory, where the holographic baryon is expressed as an Abrikosov vortex. We numerically calculate the baryon solution of holographic QCD using a fine and large lattice, keeping background gravity from the N_c D4-brane.

In addition, we investigate a various-size baryon and the dilatation mode (time-dependent size-oscillation) of a single baryon, using the relation between the baryon size and the zero-point location of the Higgs field in the reduced Abelian Higgs theory.

This size oscillation is physically considered as a collective motion and is difficult to be described in the quark model. Instead, the size oscillation mode has been studied in the Skyrmion research, and its lowest excitation mode is identified as the Roper resonance $\mathrm{N}^*(1440)$ [25–31].

The Roper resonance is the first excited state of the nucleon N(940) with the positive parity and its energy being 1440 MeV. In the quark model, based on the single-particle picture, the first excited-state baryon is to have negative parity, and it contradicts the experimental data. In lattice QCD, the numerical results with overlap fermion well reproduce the Roper resonance in terms of the excitation energy and the positive parity [32,33]. Here, lattice QCD is a powerful tool for the quantitative analysis of hadrons, but it is difficult to get state information of hadrons like the wave function due to path integral formalism, where all the states are integrated out. As an alternative method, the Skyrme model seems to succeed to reproduce the mass and parity of $\mathrm{N}^*(1440)$ as the first excited state of N(940). In this chiral soliton picture, this first excited state is described as a dilatation or breathing mode of the ground-state soliton [26–31].

Therefore, we here investigate the dilatation mode of the baryon in holographic QCD and finally compare it with the Roper resonance $\mathrm{N}^*(1440)$ in terms of its mass and parity. The dilatation mode of baryon can be described also in holographic QCD. Note again that the Sakai-Sugimoto model reduces into the Skyrme model, when massive mesons except for pions are dropped off. In fact, the holographic baryon appears as a soliton [16,19], i.e., a spatially extended object, and therefore has dilatation mode. Note, however, that holographic dilatation is four-dimensional spatial oscillation including the extra spatial dimension rather than ordinary three-dimensional one.

The organization of this paper is as follows. In Sec. II, we briefly review the Sakai-Sugimoto model as typical holographic QCD. In Sec. III, we apply the Witten Ansatz in holographic QCD. Owing to the Witten Ansatz, the $1+4$ dimensional Yang-Mills theory reduces into a $1+2$ dimensional Abelian Higgs theory. In Sec. IV, using the Witten Ansatz, we present the vortex description of baryons in holographic QCD, and we numerically obtain the ground-state solution of the holographic baryon using a fine and large-volume lattice. In Sec. V, we numerically analyze size dependence of the holographic baryon. In Sec. VI, we investigate time-dependent dilatational modes of a single baryon in holographic QCD. Section VII is devoted for summary and conclusion.

II. HOLOGRAPHIC QCD ACTION IN THE SAKAI-SUGIMOTO MODEL

In this section, as a starting point, we introduce the Sakai-Sugimoto model, one of the most successful holographic QCD [5]. In the Sakai-Sugimoto model, four-dimensional massless QCD is constructed using the $\mathrm{D4/D8/\overline{D8}}$ multi-D-brane system, which comprises spatially S^1-compactified N_c D4 branes attached with N_f D8-$\overline{\mathrm{D8}}$ pairs. Here, N_c means the color number, and N_f the light flavor number. This compactification breaks SUSY due to the (anti)periodic conditions for bosons(fermions), as was demonstrated for a D4 brane system by Witten [3]. The compactification radius is M_{KK}^{-1}, and this model parameter physically corresponds to a UV cutoff in holographic QCD. This system is infrared equivalent to massless QCD, where chiral symmetry exists [5]. Using AdS/CFT correspondence (gauge/gravity duality), the N_c D4 branes are transformed into a gravitational source, and the system becomes N_f D8 branes in the D4 gravity background, which leads to the DBI and CS action at the leading order of $1/N_c$ within the probe approximation. In terms of $1/\lambda$ expansion, the DBI action includes its leading order, and the CS action is subleading.

From the multi-D-brane system which is infrared equivalent to massless QCD, the DBI action becomes $1+4$ dimensional Yang-Mills theory on the flavor space of $\mathrm{U}(N_f)\simeq \mathrm{SU}(N_f)\times \mathrm{U}(1)$ at the leading order of $1/\lambda$ expansion [5]:

$$\begin{aligned} S_{\mathrm{5YM}} &= S_{\mathrm{5YM}}^{\mathrm{SU}(N_f)} + S_{\mathrm{5YM}}^{\mathrm{U}(1)} \\ &= -\kappa\int d^4x dw\, \mathrm{tr}\left[\frac{1}{2}h(w)F_{\mu\nu}F^{\mu\nu} + k(w)F_{\mu w}F^{\mu w}\right] \\ &\quad -\frac{\kappa}{2}\int d^4x dw\left(\frac{1}{2}h(w)\hat{F}_{\mu\nu}\hat{F}^{\mu\nu} + k(w)\hat{F}_{\mu w}\hat{F}^{\mu w}\right). \end{aligned} \quad (1)$$

In this paper, we use w for the extra fifth-coordinate in holographic QCD. $\hat{A}$ denotes U(1) gauge field and $\hat{F}$ U(1) field strength [34].

For $M, N = t, x, y, z, w$, the field strengths are given by

$$\begin{aligned} F_{MN} &\equiv \partial_M A_N - \partial_N A_M + i[A_M, A_N], \\ \hat{F}_{MN} &\equiv \partial_M \hat{A}_N - \partial_N \hat{A}_M, \end{aligned} \quad (2)$$

with the five-dimensional $\mathrm{SU}(N_f)$ gauge field $A^M(x^\mu, w)$ and U(1) gauge field $\hat{A}^M(x^\mu, w)$, respectively. Throughout this paper, we take the $M_{\mathrm{KK}} = 1$ unit together with the natural unit, and κ is written as $\kappa = \frac{\lambda N_c}{216\pi^3}$ in this unit. Note that, as a relic of N_c D4-branes, there appear background gravity $k(w)$ and $h(w)$ depending on the extra fifth-coordinate w,

$$k(w) \equiv 1 + w^2, \qquad h(w) \equiv k(w)^{-1/3}, \quad (3)$$

in the $M_{\mathrm{KK}} = 1$ unit. In Eq. (1) at the leading order of $1/\lambda$ expansion, $\mathrm{SU}(N_f)$ variables A and U(1) variables $\hat{A}$ are completely separated, and hence we have divided S_{5YM} into the $\mathrm{SU}(N_f)$ sector $S_{\mathrm{5YM}}^{\mathrm{SU}(N_f)}$ and the U(1) sector $S_{\mathrm{5YM}}^{\mathrm{U}(1)}$.

The $1/N_c$-leading holographic QCD also has the CS term [5,19] as the next leading order of $1/\lambda$. The CS term is a topological term responsible for anomalies in QCD, and its explicit form is

$$S_{\rm CS} = \frac{N_c}{24\pi^2}\int \omega_5(\mathcal{A}) = \frac{N_c}{24\pi^2}\int {\rm tr}\left(\mathcal{A}\mathcal{F}^2 - \frac{i}{2}\mathcal{A}^3\mathcal{F} - \frac{1}{10}\mathcal{A}^5\right), \quad (4)$$

where $\mathcal{A} = A + \frac{1}{\sqrt{2N_f}}\hat{A}$ denotes the $\mathrm{U}(N_f)$ gauge field [5]. Note that $\mathrm{SU}(N_f)$ variables A and U(1) variables $\hat{A}$ are dynamically mixed in the CS term $S_{\rm CS}$ in Eq. (4).

In this paper, to analyze baryons in holographic QCD, we consider both Yang-Mills and CS parts for the case of $N_f = 2$.

III. WITTEN ANSATZ IN HOLOGRAPHIC QCD

Holographic QCD is formulated to be a $1+4$ dimensional $\mathrm{U}(N_f)$ non-Abelian gauge theory with a gravitational background $h(w)$ and $k(w)$, which would be fairly difficult to analyze. To avoid the difficulty and to proceed analytic calculations, most previous works [19–21] were forced to take a flat background $h(w) = k(w) = 1$ and to use the simple 't Hooft instanton solution [35,36] in the flat space, although $h(w)$ and $k(w)$ are the trace of D4-branes and are to be relevant ingredients.

To deal with holographic QCD for $N_f = 2$ without reduction the gravitational backgrounds $h(w)$ and $k(w)$, we adopt the Witten Ansatz [37] in this paper. The Witten Ansatz is generally applicable for spatially-rotational symmetric system in the SU(2) Yang-Mills theory. Applying this to holographic QCD, the $1+4$ dimensional non-Abelian theory transforms to a $1+2$ dimensional Abelian Higgs theory. Accordingly, relevant topological objects are changed from instantons to vortices, as will be shown in Sec. IV. In this section, we generalize the Witten Anstaz to be applicable to holographic QCD.

A. Witten Ansatz for Euclidean Yang-Mills theory

In this subsection, we briefly review the original Witten Ansatz [37] applied for the Euclidean four-dimensional SU(2) Yang-Mills theory, which is formulated on three spatial coordinates (x, y, z) and Euclidean time t. For spatially rotational symmetric systems, the Witten Ansatz can be applied as

$$A_i^a(x,y,z,t) = \frac{\phi_2(r,t)+1}{r}\epsilon_{iak}\hat{x}_k + \frac{\phi_1(r,t)}{r}\hat{\delta}_{ia} + a_r(r,t)\hat{x}_i\hat{x}_a, \quad (5)$$

$$A_t^a(x,y,z,t) = a_t(r,t)\hat{x}^a \quad (6)$$

with $r \equiv (x_i x_i)^{1/2}$, $\hat{x}_i \equiv x_i/r$ and $\hat{\delta}_{ij} \equiv \delta_{ij} - \hat{x}_i\hat{x}_j$.

Using the Witten Ansatz, the four-dimensional SU(2) Yang-Mills theory is reduced into a two-dimensional Abelian Higgs theory as

$$S_{\rm YM}^{\rm SU(2)} = \int dt d^3x \frac{1}{2}{\rm tr}F_{\mu\nu}F^{\mu\nu} = 4\pi\int_{-\infty}^{\infty}dt\int_0^{\infty}dr\left[|D_0\phi|^2 + |D_1\phi|^2 + \frac{1}{2r^2}(1-|\phi|^2)^2 + \frac{r^2}{2}f_{01}^2\right], \quad (7)$$

where the complex Higgs field $\phi(t,r)$, Abelian gauge field $a_\mu(t,r)$, its covariant derivative D_μ, and field strength $f_{\mu\nu}$ in the Abelian Higgs theory are

$$\phi \equiv \phi_1 + i\phi_2 \in \mathbf{C}, \qquad a_\mu \equiv (a_0, a_1),$$
$$D_\mu \equiv \partial_\mu - ia_\mu, \qquad f_{01} \equiv \partial_0 a_1 - \partial_1 a_0. \quad (8)$$

Here, we have used $(0,1) = (t,r)$ for the index of two dimensional coordinates.

B. Generalized Witten Ansatz for $\mathrm{SU}(2)_f$ sector in holographic QCD

In this subsection, we generalize the Witten Ansatz to be applicable for holographic QCD.

The $\mathrm{SU}(2)_f$ sector in holographic QCD is expressed as a $1+4$ dimensional Yang-Mills theory with gravitational backgrounds $h(w)$ and $k(w)$. Holographic QCD already includes four-dimensional Euclidean spatial coordinates (x, y, z, w) including the extra fifth-coordinate w, and instantons can be naturally introduced in holographic QCD without necessity of the Euclidean process or the Wick rotation.

Describing the $\mathrm{SU}(2)_f$ gauge field A with the Pauli matrix τ^a as $A = A^a\frac{\tau^a}{2} \in \mathrm{su}(2)_f$ in holographic QCD, we take a generalized version of the Witten Ansatz for (x,y,z)-spatially rotational symmetric systems [23,24,34],

$$A_0^a(t,x,y,z,w) = a_0(t,r,w)\hat{x}^a, \quad (9)$$

$$A_i^a(t,x,y,z,w) = \frac{\phi_2(t,r,w)+1}{r}\epsilon_{iak}\hat{x}^k + \frac{\phi_1(t,r,w)}{r}\hat{\delta}_{ia} + a_r(t,r,w)\hat{x}_i\hat{x}_a, \quad (10)$$

$$A_w^a(t,x,y,z,w) = a_w(t,r,w)\hat{x}^a, \quad (11)$$

with $r \equiv (x_i x_i)^{1/2}$, $\hat{x}_i \equiv x_i/r$ and $\hat{\delta}_{ij} \equiv \delta_{ij} - \hat{x}_i\hat{x}_j$. For $1+4$ dimensional holographic QCD, we have extended the Witten Ansatz for A_0^a component, considering the (x,y,z)-rotational symmetry. Note that this Ansatz is a general form when (x,y,z)-rotational symmetry is imposed on gauge fields.

In the Witten Ansatz, the holographic field strength, F_{ij}, F_{0i}, F_{wi} and F_{0w} are expressed as

$$\frac{1}{2}\varepsilon_{ijk}F^a_{jk} = (\partial_1\phi_2 - a_1\phi_1)\frac{\hat{\delta}_{ai}}{r} + (1-\phi_1^2-\phi_2^2)\frac{\hat{x}_a\hat{x}_i}{r^2} + (\partial_1\phi_1 + a_1\phi_2)\frac{1}{r}\varepsilon_{aik}\hat{x}_k \tag{12}$$

$$F^a_{0i} = (\partial_0\phi_1 + a_0\phi_2)\frac{\hat{\delta}_{ai}}{r} + (\partial_0 a_1 - \partial_1 a_0)\hat{x}_a\hat{x}_i - (\partial_0\phi_2 - a_0\phi_1)\frac{1}{r}\varepsilon_{aik}\hat{x}_k \tag{13}$$

$$F^a_{wi} = (\partial_2\phi_1 + a_2\phi_2)\frac{\hat{\delta}_{ai}}{r} + (\partial_2 a_1 - \partial_1 a_2)\hat{x}_a\hat{x}_i - (\partial_2\phi_2 - a_2\phi_1)\frac{1}{r}\varepsilon_{aik}\hat{x}_k \tag{14}$$

$$F^a_{0w} = (\partial_0 a_2 - \partial_2 a_0)\hat{x}^a. \tag{15}$$

With the Witten Ansatz, $1+4$ dimensional $\mathrm{SU}(2)_f$ Yang-Mills sector of holographic QCD is reduced into a $1+2$ dimensional Abelian Higgs theory on a curved space. In fact, $S_{5\mathrm{YM}}^{\mathrm{SU}(2)_f}$ is rewritten as

$$\begin{aligned} S_{5\mathrm{YM}}^{\mathrm{SU}(2)_f} &= -\kappa\int d^4x dw \,\mathrm{tr}\left[\frac{1}{2}h(w)F_{\mu\nu}F^{\mu\nu} + k(w)F_{\mu w}F^{\mu w}\right] \\ &= 4\pi\kappa\int_{-\infty}^{\infty}dt\int_0^{\infty}dr\int_{-\infty}^{\infty}dw\Big[h(w)(|D_0\phi|^2 - |D_1\phi|^2) \\ &\quad - k(w)|D_2\phi|^2 - \frac{h(w)}{2r^2}(1-|\phi|^2)^2 \\ &\quad + \frac{r^2}{2}\{h(w)f_{01}^2 + k(w)f_{02}^2 - k(w)f_{12}^2\}\Big], \end{aligned} \tag{16}$$

where the complex Higgs field $\phi(t,r,w)\in\mathbf{C}$, Abelian gauge field $a_\mu(t,r,w)$, its covariant derivative D_μ, and field strength $f_{\mu\nu}$ in the Abelian Higgs theory are

$$\begin{aligned} &\phi \equiv \phi_1 + i\phi_2 \in \mathbf{C}, \qquad a_\mu \equiv (a_0, a_r, a_w), \\ &D_\mu \equiv \partial_\mu - i a_\mu, \qquad f_{\mu\nu} \equiv \partial_\mu a_\nu - \partial_\nu a_\mu. \end{aligned} \tag{17}$$

Here, we have used $(0,1,2) = (t,r,w)$ for the index of $1+2$ dimensional coordinates. Note that the factor $k(w)$ appears in D_2 and F_{12} associated with the index 2 (w), and otherwise the factor $h(w)$ appears.

From this action, the static energy of the Yang-Mills part is obtained as

$$\begin{aligned} &E_{5\mathrm{YM}}^{\mathrm{SU}(2)_f}[\phi(r,w), \vec{a}(r,w)] \\ &= 4\pi\kappa\int_0^{\infty}dr\int_{-\infty}^{\infty}dw\Big[h(w)|D_1\phi|^2 + k(w)|D_2\phi|^2 \\ &\quad + \frac{h(w)}{2r^2}\{1-|\phi|^2\}^2 + \frac{r^2}{2}k(w)f_{12}^2\Big] \\ &= 4\pi\int_0^{\infty}dr r^2\int_{-\infty}^{\infty}dw\,\mathcal{E}^{\mathrm{SU}(2)_f}(r,w), \end{aligned} \tag{18}$$

with $\vec{a} = (a_1, a_2) = (a_r, a_w)$. This is similar with the $1+2$ dimensional Ginzburg-Landau theory. As the different point, however, there appears a nontrivial metric of r^2 [37] in addition to holographic background gravity of $h(w)$ and $k(w)$ in the (r,w) half plane. To include all the gravitational effects exactly, we construct the lattice formalism, as shown in Appendix A, and perform the numerical calculation for holographic QCD.

Finally in the subsection, we investigate the topological density ρ_B in the Witten Ansatz. For the $\mathrm{SU}(2)_f$ gauge configuration in the Witten Ansatz, the topological density ρ_B in (x,y,z,w)-space is found to be [34]

$$\begin{aligned} \rho_B &\equiv \frac{1}{16\pi^2}\mathrm{tr}(F_{MN}\tilde{F}_{MN}) = \frac{1}{32\pi^2}\epsilon_{MNPQ}\mathrm{tr}(F_{MN}F_{PQ}) \\ &= \frac{1}{8\pi^2r^2}\{-i\epsilon_{ij}(D_i\phi)^*D_j\phi + \epsilon_{ij}\partial_i a_j(1-|\phi|^2)\} \\ &= \frac{1}{8\pi^2r^2}\epsilon_{ij}\partial_i\left\{\frac{1}{2i}(\phi^*\partial_j\phi - \phi\partial_j\phi^*) + a_j(1-|\phi|^2)\right\} \\ &= \frac{1}{8\pi^2r^2}\epsilon_{ij}\partial_i\{a_j(1-|\phi|^2) + \partial_j\theta\cdot|\phi|^2\}, \end{aligned} \tag{19}$$

where $\theta \equiv \arg\phi$ and Roman small letters i, j take $(1,2) = (r,w)$. The topological density ρ_B is expressed as a total derivative. Since we consider (x,y,z)-rotationally symmetric system, ρ_B is independent of the spatial direction $(\hat{x},\hat{y},\hat{z})$. In fact, ρ_B takes an SO(3) rotationally symmetric form of $\rho_B(r,w)$ in the second line of Eq. (19).

C. U(1) sector in holographic QCD

In this subsection, we consider the U(1) sector in holographic QCD. Hereafter, the capital-letter index denotes the Euclidean spatial index as $M = x$, y, z, w. Also for the U(1) gauge field $\hat{A}$, we respect the spatial SO(3) rotational symmetry [23,24] as in the Witten Ansatz, and impose

$$\hat{A}_i(t,x,y,z,w) = \hat{a}_r(t,r,w)\hat{x}_i, \tag{20}$$

while $\hat{A}_0$ and $\hat{A}_w$ are treated to be arbitrary. In this case, one finds $\hat{F}_{ij} = 0$ and can take the $\hat{a}_r = 0$ gauge, which simplifies $\hat{A}_i = 0$.

Then, the $1/\lambda$-leading term $S_{5\mathrm{YM}}^{\mathrm{U}(1)}$ for the U(1) gauge field is written as [34]

$$S^{\mathrm{U}(1)} = \frac{\kappa}{2}\int d^4x dw\{h(w)\hat{F}_{0i}^2 + k(w)\hat{F}_{0w}^2 - k(w)\hat{F}_{iw}^2\}$$
$$= \int d^4x dw\left[\frac{1}{2}\hat{A}_0 K\hat{A}_0 - \frac{\kappa}{2}k(w)(\partial_i\hat{A}_w)^2 + (\text{time-derivative terms})\right], \tag{21}$$

using the SO(3)-symmetric non-negative Hermite kernel

$$K \equiv -\kappa\{h(w)\partial_i^2 + \partial_w k(w)\partial_w\}$$
$$= -\kappa\left\{h(w)\frac{1}{r^2}\partial_r r^2\partial_r + \partial_w k(w)\partial_w\right\}. \tag{22}$$

In this calculation, we take $\hat{A}_i = 0$ using the gauge and rotational symmetry.

We consider the CS term S_{CS} as the next leading order of the $1/\lambda$ expansion. For the static SO(3)-rotationally symmetric configuration in the $A_0 = 0$ gauge, the CS term S_{CS} in Eq. (4) is transformed as [19,23,24,34]

$$S_{\mathrm{CS}} = \frac{N_c}{24\pi^2}\epsilon_{MNPQ}\int d^4x dw\left[\frac{3}{8}\hat{A}_0\mathrm{tr}(F_{MN}F_{PQ}) - \frac{3}{2}\hat{A}_M\mathrm{tr}(\partial_0 A_N F_{PQ}) + \frac{3}{4}\hat{F}_{MN}\mathrm{tr}(A_0 F_{PQ}) + \frac{1}{16}\hat{A}_0\hat{F}_{MN}\hat{F}_{PQ} - \frac{1}{4}\hat{A}_M\hat{F}_{0N}\hat{F}_{PQ}\right]$$
$$= \frac{N_c}{2}\int d^4x dw \rho_B\hat{A}_0, \tag{23}$$

up to total derivative. This is Coulomb-type interaction between the U(1) gauge potential $\hat{A}_0$ and the topological density $\rho_B \equiv \frac{1}{16\pi^2}\mathrm{tr}(F_{MN}\tilde{F}_{MN})$.

Then, the total U(1) action depending on the U(1) gauge field $\hat{A}$ is written as

$$S^{\mathrm{U}(1)} \equiv S^{\mathrm{U}(1)} + S_{\mathrm{CS}}$$
$$= \int d^4x dw\left[\frac{1}{2}\hat{A}_0 K\hat{A}_0 + \frac{N_c}{2}\rho_B\hat{A}_0 - \frac{\kappa}{2}k(w)(\partial_i\hat{A}_w)^2\right], \tag{24}$$

which leads to the field equations,

$$K\hat{A}_0 + \frac{N_c}{2}\rho_B = 0, \qquad \partial_i^2\hat{A}_w = 0. \tag{25}$$

For the static configuration, the additional energy $E^{\mathrm{U}(1)}$ from U(1) sector $S^{\mathrm{U}(1)}$ is simply given by

$$E^{\mathrm{U}(1)} = -S^{\mathrm{U}(1)}/\int dt$$
$$= \int d^3x dw\left[-\frac{1}{2}\hat{A}_0 K\hat{A}_0 - \frac{N_c}{2}\rho_B\hat{A}_0 + \frac{\kappa}{2}k(w)(\partial_i\hat{A}_w)^2\right]. \tag{26}$$

For the static case, $\hat{A}_w$ is dynamically isolated in the field equation (25) and the last term is non-negative in the energy (26), and therefore we set $\hat{A}_w = 0$, which satisfies the local energy-minimum condition. Then, one finds

$$E^{\mathrm{U}(1)} = -\int d^3x dw\left[\frac{1}{2}\hat{A}_0 K\hat{A}_0 + \frac{N_c}{2}\rho_B\hat{A}_0\right]. \tag{27}$$

For the SO(3) rotationally symmetric solution, we eventually obtain the static energy of the U(1) part:

$$E^{\mathrm{U}(1)}[\rho_B(r,w),\hat{A}_0(r,w)] = -4\pi\int_0^\infty dr r^2\int_{-\infty}^\infty dw\left[\frac{1}{2}\hat{A}_0(r,w)K\hat{A}_0(r,w) + \frac{N_c}{2}\rho_B(r,w)\hat{A}_0(r,w)\right]$$
$$= -\int_0^\infty dr\int_{-\infty}^\infty dw\left[\frac{1}{2}\hat{A}_0(r,w)\tilde{K}\hat{A}_0(r,w) + 2\pi N_c\tilde{\rho}_B(r,w)\hat{A}_0(r,w)\right]$$
$$= 4\pi\int_0^\infty dr r^2\int_{-\infty}^\infty dw\mathcal{E}^{\mathrm{U}(1)}(r,w), \tag{28}$$

using $\tilde{\rho}_B(r,w) \equiv r^2\rho_B(r,w)$ and the Hermite kernel $\tilde{K}$ in (r,w)-space,

$$\tilde{K} \equiv 4\pi r^2 K = -4\pi\kappa\{h(w)\partial_r r^2\partial_r + r^2\partial_w k(w)\partial_w\}. \tag{29}$$

For the numerical calculation of the U(1) sector, we mainly use this energy functional. (For another expression of $E^{\mathrm{U}(1)}$ after $\hat{A}^0$ path-integration, see Appendix B.)

Note again that, at the leading order of $1/\lambda$, the U(1) sector ($\hat{A}$) completely decouples with the $\mathrm{SU}(2)_f$ sector ($\vec{a}$, ϕ) because the leading term is only the Yang-Mills action (1). However, at the next leading order of $1/\lambda$, the U(1) term affects the $\mathrm{SU}(2)_f$ part through the CS term as Eq. (23).

To summarize, the total energy E comprises two parts,

$$E[\phi(r,w),\vec{a}(r,w),\hat{A}_0(r,w)]$$
$$= E_{5\mathrm{YM}}^{\mathrm{SU}(2)_f}[\phi,\vec{a}] + E^{\mathrm{U}(1)}[\rho_B,\hat{A}_0], \tag{30}$$

and the total energy density $\mathcal{E}(r,w)$ is written as

$$\mathcal{E}(r,w) = \mathcal{E}^{\mathrm{SU}(2)_f}(r,w) + \mathcal{E}^{\mathrm{U}(1)}(r,w), \tag{31}$$

and we have to deal with coupled field equations of the $\mathrm{SU}(2)_f$ and U(1) sectors and will perform the numerical calculation in a consistent manner.

IV. VORTEX DESCRIPTION OF BARYONS

In this section, we introduce vortex description of baryons in holographic QCD with applying the generalized Witten Ansatz. For a single baryon which is (x,y,z)-spatially rotational symmetric, applying the Witten Ansatz, we reduce the theory into a $1+2$ dimensional Abelian Higgs theory in a curved space. In the reduced theory, the holographic baryon is expressed as a two-dimensional topological object of an Abrikosov vortex. We perform the numerical calculation of a $B=1$ solution of holographic QCD as the single ground-state baryon, using a fine and large lattice with spacing of 0.04 fm and size of 10 fm.

A. Holographic baryons in Witten Ansatz

Large N_c analyses of QCD indicate that explicit degree of freedoms are only mesons and glueballs, and baryons appear as solitons (topological objects) constructed with meson fields [12]. Also, holographic QCD based on large N_c becomes an effective theory of mesons, and baryons appear as chiral solitons composed of meson fields in this framework [5,16]. Holographic QCD has four dimensional space (x,y,z,w), and instantons naturally appear as relevant topological objects in the four-dimensional space. The topological objects are physically identified as baryons in holographic QCD [19] and called holographic baryons.

Remarkably, the Witten Ansatz generally converts the topological description from a four-dimensional instanton into a two-dimensional vortex [37]. Accordingly, the vortex number is interpreted as the baryon number in holographic QCD with the Witten Ansatz [34].

In fact, the baryon number B or the Pontryagin index is written by a contour integral in the (r,w)-plane

$$\begin{aligned} B &= \int d^3x dw \rho_B \\ &= \frac{1}{2\pi}\int_0^\infty dr \int_{-\infty}^{\infty} dw \epsilon_{ij}\partial_i\{a_j(1-|\phi|^2) + \partial_j\theta\cdot|\phi|^2\} \\ &= \oint_{r\geq 0} d\mathbf{s}\cdot\{\mathbf{a}(1-|\phi|^2) + \nabla\theta\cdot|\phi|^2\} \\ &= \oint_{r\geq 0} d\mathbf{s}\cdot\nabla\theta, \end{aligned} \tag{32}$$

where $\oint_{r\geq 0}$ denotes the contour integral around the whole half-plane of (r,w) with $r\geq 0$. To keep the energy (18) finite, we have imposed the following boundary conditions:

$$|\phi(r=0, {}^\forall w)| = 1, \tag{33}$$

$$|\phi({}^\forall r, w=\pm\infty)| = |\phi(r=\infty, {}^\forall w)| = 1, \tag{34}$$

at the edge of the (r,w) half-plane. Thus, the baryon number B is converted into the vortex number in this formalism [34].

B. Abrikosov vortex solution for a baryon in holographic QCD

In this subsection, we numerically calculate a ground-state baryon of holographic QCD through the Abrikosov vortex description in the $1+2$ dimensional U(1) Abelian Higgs theory [34].

With imposing the global condition of $B=1$, we numerically minimize the total energy $E[\phi,\vec{a},\hat{A}_0]$ in Eq. (30), which is equivalent to solving the equation of motion (EOM) of holographic QCD for the single ground-state baryon.

Regarding the two parameters M_{KK} and κ in holographic QCD, we take $M_{\mathrm{KK}}\simeq 948$ MeV, and $\kappa = 7.46\times 10^{-3}$ to reproduce $f_\pi \simeq 92.4$ MeV and $m_\rho \simeq 776$ MeV [5,16]. In this study, we have used the Kaluza-Klein unit of $M_{\mathrm{KK}}=1$.

For the numerical calculation on the (r,w) plane, we adopt a fine and large-size lattice with spacing of $0.2\ M_{\mathrm{KK}}^{-1}\simeq 0.04$ fm and the extension of $0\leq r\leq 250$ and $-125\leq w\leq 125$, that is, the system size is 250×250 grid corresponding to $(50\ M_{\mathrm{KK}}^{-1})^2 \simeq (10\ \mathrm{fm})^2$ in the physical unit. (In this numerical calculation, there appears subtle cancellation, and use of a coarse lattice might lead to an inaccurate result. Also, the lattice size should be increased until the volume dependence of physical quantities disappears.)

On this lattice, starting from the 't Hooft solution [35,36] as a $B=1$ topological configuration, we numerically perform minimization of the total energy $E[\phi,\vec{a},\hat{A}_0]$ keeping the topological charge by an iterative improvement, that is, many-time iterative local replacements of the field variable of ϕ, $\vec{a}$ and $\hat{A}_0$. (See Appendix A for the detail.) During the update, the Higgs field $\phi(x)$ always has a zero point to ensure $B=1$, and the Higgs zero-point generally moves so as to realize the ground state. In this way, we eventually obtain the holographic fields $\phi(r,w)$, $\vec{a}(r,w)$ and $\hat{A}_0(r,w)$ for the ground-state baryon as the true solution of EOM in holographic QCD.

For the confirmation of numerical calculations, we also consider another different method, as shown in Appendix B. In this alternative method, we integrate out the U(1) gauge field $\hat{A}_0$ and update only $\phi(r,w)$ and $\vec{a}(r,w)$ on the lattice based on Eq. (B2). We have confirmed that both methods give the same numerical results for holographic baryons.

To visualize gauge and Higgs fields composing the Abrikosov vortex, we take the Landau gauge for the U(1) gauge degrees of freedom, $\partial_i a_i(r,w)=0$. Of course, main results including the total energy are gauge invariant and never depend on any gauge choices.

For the single ground-state baryon, we show field configurations $\phi(r,w)$ and $\vec{a}(r,w)$ in Fig. 1, and also the U(1) gauge field $\hat{A}_0(r,w)$ in Fig. 2. The Higgs field $\phi(r,w)$ indicates a clear topological structure characterizing the Abrikosov vortex, which is mapped into an instanton [37] via the Witten Ansatz and physically means a baryon in holographic QCD [23,34]. In accordance with the field equation (25), $\hat{A}_0$ is localized around the nonvanishing topological density ρ_B, which will be shown in Fig. 3.

Quantitatively, unlike the initial ’t Hooft solution, Fig. 1 no longer indicates the symmetry between r and w for the ground-state baryon solution in holographic QCD. For the ground-state baryon, both profiles of ϕ and $\vec{a}$ are found to be a little shrink in the w direction, compared with four-dimensional spherical ’t Hooft solutions, which was also found in the previous numerical studies [23,24,34].

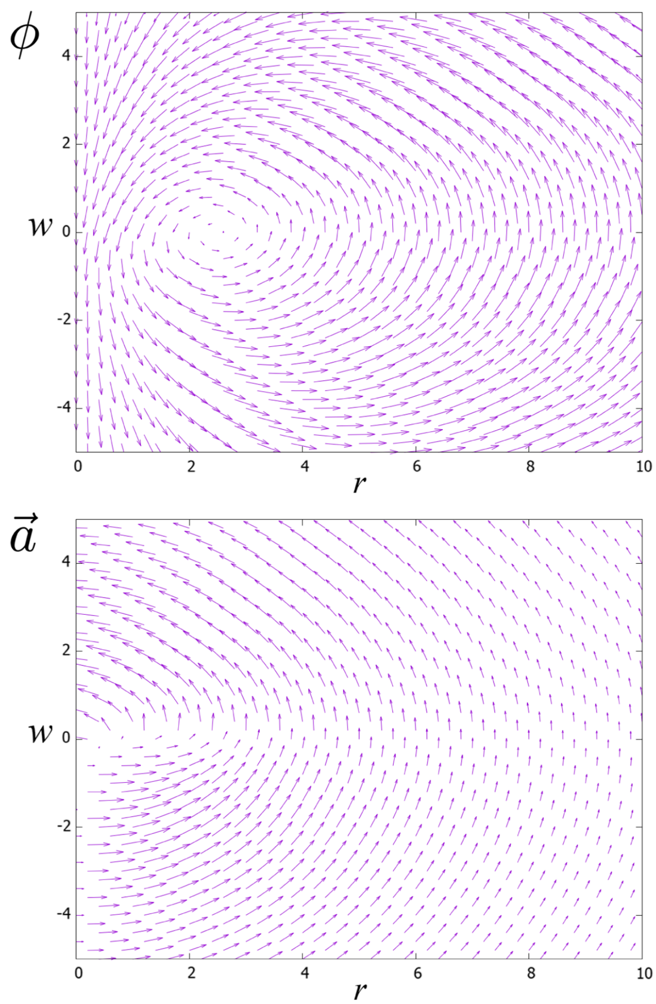

FIG. 1. Vortex description for the single ground-state baryon: the Higgs field $\phi(r,w) = (\mathrm{Re}[\phi], \mathrm{Im}[\phi])$ (upper) and the Abelian gauge field $a(r,w) = (a_1, a_2)$ (lower) in the Landau gauge. The Kaluza-Klein unit of $M_{\mathrm{KK}} = 1$ is used. The Higgs field has a zero point at $(r,w) \simeq (2.4, 0)$, and its winding number around the zero point is equal to the baryon number, that is, $B = 1$.

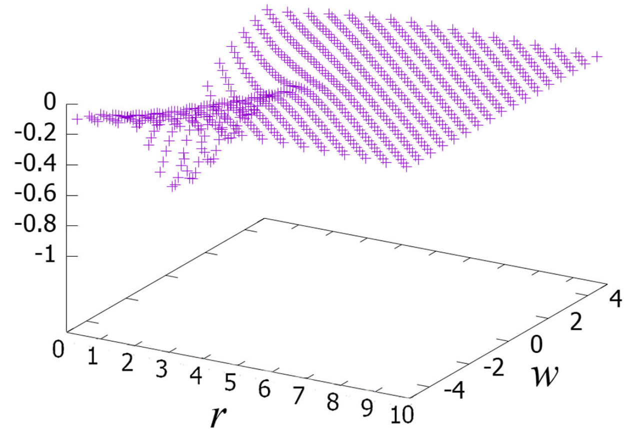

FIG. 2. Temporal component of the U(1) gauge field $\hat{A}_0(r,w)$ in the ground-state holographic baryon in the $M_{\mathrm{KK}} = 1$ unit. This U(1) gauge field $\hat{A}_0$ directly interacts with the topological density ρ_B and leads to a repulsive force between topological densities, like the Coulomb interaction in QED.

C. Properties of the ground-state baryon in holographic QCD

Now, we show the properties of the ground-state baryon in holographic QCD, which is numerically calculated by

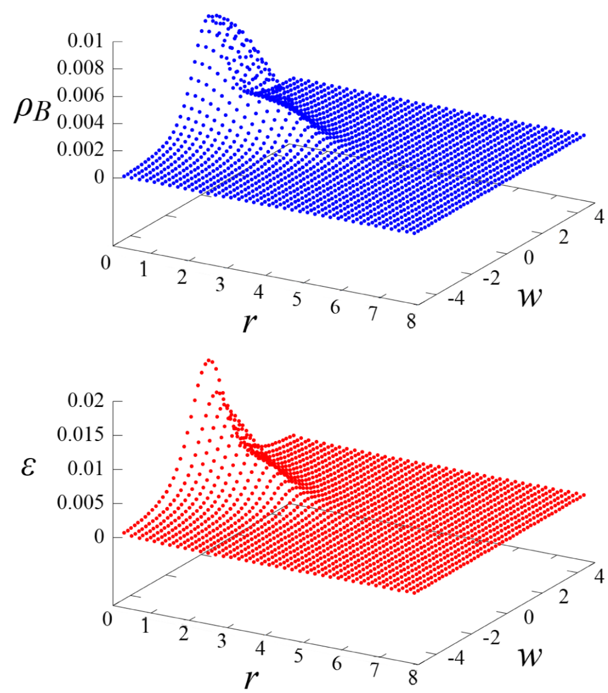

FIG. 3. Topological density $\rho_B(r,w)$ (upper) and total energy density $\mathcal{E}(r,w)$ (lower) for the ground-state solution of a single holographic baryon in the $M_{\mathrm{KK}} = 1$ unit. Both densities have a peak around $(r,w) = (0,0)$.

minimizing the total energy $E[\phi, \vec{a}, \hat{A}_0]$ in Eq. (30). In Fig. 3, we show the topological density $\rho_B(r,w)$ and total energy density $\mathcal{E}(r,w)$ in the (r,w)-plane for the Abrikosov vortex solution in the $1+2$ dimensional Abelian Higgs theory. Both densities have a peak around $(r,w) = (0,0)$ and are extended in both the r and w directions. We show in Fig. 4 the densities multiplied by the integral measure factor r^2, i.e., $4\pi r^2 \rho_B(r,w)$ and $4\pi r^2 \mathcal{E}(r,w)$, for the ground-state baryon, since $\tilde{\rho}_B(r,w) \equiv r^2 \rho_B(r,w)$ is a primary variable in this numerical calculation, as shown in Eq. (29). The nonzero size of the baryon is due to the repulsive force from the CS term [19].

In general, the integrated topological density is the baryon number B, and the baryon mass M_B is given by integration of the total energy density $\mathcal{E}(r,w)$:

$$B = \int d^3x dw \rho_B(r,w) = 4\pi \int_0^\infty dr r^2 \int_{-\infty}^\infty dw\, \rho_B(r,w), \tag{35}$$

$$M_B = \int d^3x dw \mathcal{E}(r,w) = 4\pi \int_0^\infty dr r^2 \int_{-\infty}^\infty dw\, \mathcal{E}(r,w). \tag{36}$$

By integration over the extra coordinate w, we obtain the ordinary densities in a three-dimensional space,

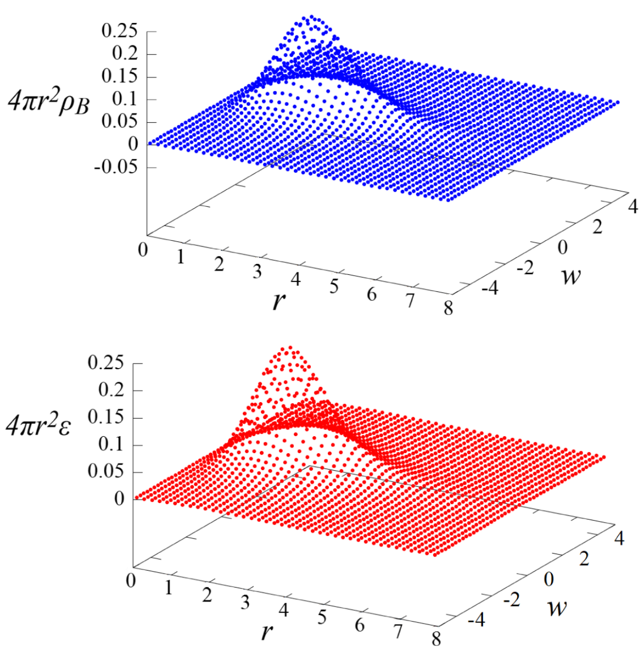

FIG. 4. r^2-multiplied topological and energy densities: $4\pi r^2 \rho_B(r,w)$ (upper) and $4\pi r^2 \mathcal{E}(r,w)$ (lower) for the ground-state solution of a single holographic baryon in the $M_{KK} = 1$ unit. Both figures have a peak around $(r,w) \simeq (2,0)$ near the vortex center, which roughly controls the baryon size.

$$\rho_B(r) \equiv \int_{-\infty}^\infty dw \rho_B(r,w), \tag{37}$$

$$\mathcal{E}(r) \equiv \int_{-\infty}^\infty dw \mathcal{E}(r,w). \tag{38}$$

The mass M_B and size for the ground-state baryon are estimated as

$$M_B = E_{5YM}^{SU(2)_f} + E^{U(1)} = \int d^3x \mathcal{E}(r) \simeq 1.25 M_{KK} \simeq 1.19 \text{ GeV}, \tag{39}$$

$$\sqrt{\langle r^2 \rangle}_{\rho_B} \equiv \sqrt{\frac{\int d^3x \rho_B(r) r^2}{\int d^3x \rho_B(r)}} \simeq 2.58\ M_{KK}{}^{-1} \simeq 0.54 \text{ fm}, \tag{40}$$

$$\sqrt{\langle r^2 \rangle}_{\mathcal{E}} \equiv \sqrt{\frac{\int d^3x \mathcal{E}(r) r^2}{\int d^3x \mathcal{E}(r)}} \simeq 2.93\ M_{KK}{}^{-1} \simeq 0.61 \text{ fm}. \tag{41}$$

Here, some cautions are commented. When the self-dual BPS-saturated 't Hooft solution [35,36] is simply used, as was done in Ref. [19], the holographic baryon has an overestimated mass $M_B^{BPS} \simeq 1.35\ M_{KK} \simeq 1.28$ GeV and a smaller radius $\sqrt{\langle r^2 \rangle_{\rho_B}^{BPS}} \simeq 2.2\ M_{KK}^{-1} \simeq 0.46$ fm, as shown in Appendix C. (Because of such an overestimation, a small value of $M_{KK} = 500$ MeV was adopted to adjust baryon masses in Ref. [19], which significantly differs from $M_{KK} \simeq 1$ GeV for the meson sector.) Another caution is the numerical accuracy, and fine and large lattices are to be used for the numerical calculation. Owing to a relatively coarse and small-size lattice, the numerical results in the previous paper [34] include about 20% error for the baryon mass and size.

Now, we investigate spatial distribution of the baryon-number and energy densities for the ground-state baryon in holographic QCD. Figure 5 shows the baryon-number density $\rho_B(r)$ (i.e., topological density) and total energy density $\mathcal{E}(r)$, and their r^2-multiplied values, $4\pi r^2 \rho_B(r)$ and $4\pi r^2 \mathcal{E}(r)$. One finds significant difference between the shapes of $\rho_B(r)$ and $\mathcal{E}(r)$ for the small r region.

Next, we investigate the energy contribution from the $SU(2)_f$ and U(1) parts, respectively. For the mass (total static energy) $M_B = E_{5YM}^{SU(2)_f} + E^{U(1)}$ of the ground-state holographic baryon, we obtain

$$E_{5YM}^{SU(2)_f} \simeq 1.00\ M_{KK} \simeq 0.95 \text{ GeV}, \tag{42}$$

$$E^{U(1)} \simeq 0.25\ M_{KK} \simeq 0.24 \text{ GeV}, \tag{43}$$

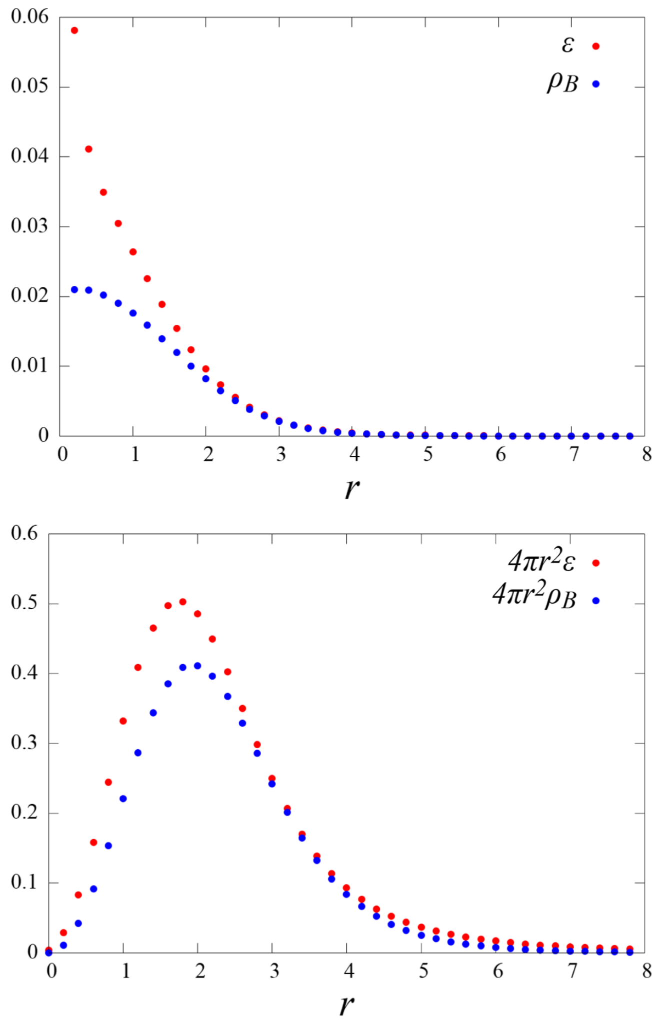

FIG. 5. Baryon density $\rho_B(r)$ and total energy density $\mathcal{E}(r)$ for the ground-state baryon. The lower panel shows $4\pi r^2\rho_B(r)$ and $4\pi r^2\mathcal{E}(r)$, including the integral measure factor r^2. Despite a significant difference between $\rho_B(r)$ and $\mathcal{E}(r)$ around the origin, this difference is reduced by the r^2 multiplication. Here, the $M_{\rm KK}=1$ unit is taken.

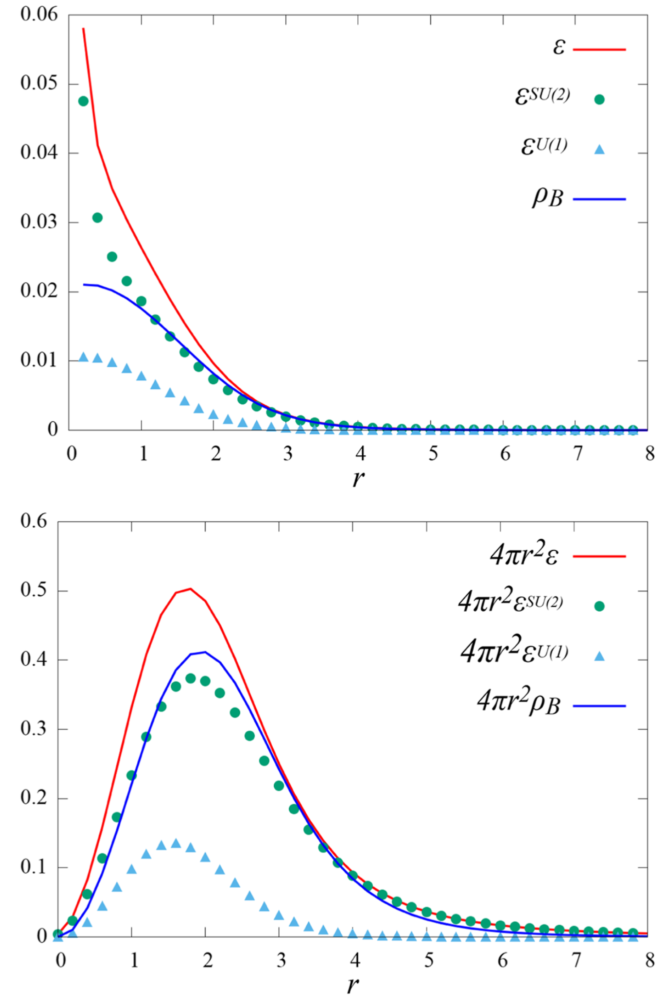

FIG. 6. $\mathrm{SU}(2)_f$ energy density $\mathcal{E}^{\mathrm{SU}(2)_f}(r)$ and U(1) energy density $\mathcal{E}^{\mathrm{U}(1)}(r)$ of the ground-state baryon, together with the total energy density $\mathcal{E}(r)$ and baryon density $\rho_B(r)$, denoted by the solid lines. The lower panel shows r^2-multiplied values, $4\pi r^2\mathcal{E}(r)$, $4\pi r^2\mathcal{E}^{\mathrm{SU}(2)_f}(r)$, $4\pi r^2\mathcal{E}^{\mathrm{U}(1)}(r)$ and $4\pi r^2\rho_B(r)$. Here, the $M_{\rm KK}=1$ unit is taken.

and hence the $\mathrm{SU}(2)_f$ contribution (leading order of $1/\lambda$ expansion) is found to be quantitatively dominant.

As spatial distribution, the $\mathrm{SU}(2)_f$ and U(1) energy densities are expressed as

$$r^2\mathcal{E}^{\mathrm{SU}(2)_f}(r)=\kappa\int_{-\infty}^{\infty}dw\bigg[h(w)|D_1\phi|^2+k(w)|D_2\phi|^2+\frac{h(w)}{2r^2}\{1-|\phi|^2\}^2+\frac{r^2}{2}k(w)f_{12}^2\bigg], \qquad (44)$$

$$\mathcal{E}^{\mathrm{U}(1)}(r)=-\int_{-\infty}^{\infty}dw\bigg[\frac{1}{2}\hat{A}_0(r,w)K\hat{A}_0(r,w)+\frac{N_c}{2}\rho_B(r,w)\hat{A}_0(r,w)\bigg]. \qquad (45)$$

Figure 6 shows $\mathrm{SU}(2)_f$ energy density $\mathcal{E}^{\mathrm{SU}(2)_f}(r)$ and U(1) energy density $\mathcal{E}^{\mathrm{U}(1)}(r)$ of the ground-state baryon, together with the total energy density $\mathcal{E}(r)$ and baryon density $\rho_B(r)$.

The dominant contribution is the $\mathrm{SU}(2)_f$ part, and the total value $\mathcal{E}(r)$ is approximated by the $\mathrm{SU}(2)_f$ energy density $\mathcal{E}^{\mathrm{SU}(2)_f}(r)$, which seems to be consistent with $1/\lambda$ expansion. In particular, $\mathcal{E}^{\mathrm{SU}(2)_f}(r)$ and $\mathcal{E}(r)$ has the same slope at the origin $r=0$ and show enhancement for small r region, although it is masked by the integral measure r^2. The shape of $\mathcal{E}^{\mathrm{U}(1)}(r)$ seems to follow $\rho_B(r)$, reflecting the direct coupling between $\hat{A}_0$ and ρ_B in the CS term (23).

Finally, we investigate self-duality breaking of the holographic baryon. The different shape between the topological and energy densities originates from the background gravity,

$h(w)$ and $k(w)$, and presence of the CS term. In the case of $h(w)=k(w)=1$ without the CS term, the instanton solution has exact self-duality of $F_{MN}=\tilde{F}_{MN}$, leading to $\rho_B(r,w)\propto\mathcal{E}(r,w)$. Hence, the functional forms of $\rho_B(r)$ and $\mathcal{E}(r)$ are forced to be the same. In fact, between the shapes of $\rho_B(r)$ and $\mathcal{E}(r)$, the similarity indicates the self-dual tendency, and the different point indicates self-duality breaking.

For the single baryon case $B=1$, we introduce the self-duality breaking parameter defined by

$$\Delta_{\rm DB}\equiv\frac{\int d^3xdw\,{\rm tr}(F_{MN}F_{MN}-F_{MN}\tilde{F}_{MN})}{\int d^3xdw\,{\rm tr}(F_{MN}\tilde{F}_{MN})}=\frac{1}{32\pi^2}\int d^3xdw\,{\rm tr}(F_{MN}-\tilde{F}_{MN})^2,\tag{46}$$

which is normalized by the topological quantity. This is non-negative and becomes zero only in the exact self-dual case. The self-duality breaking of the ground-state baryon is found to be $\Delta_{\rm DB}\simeq 0.17$, which is non-zero but seems small. The small value might indicate that the true holographic configuration is close to be self-dual. Then, the ground-state baryon might be approximated by the self-dual 't Hooft instanton in holographic QCD.

V. SIZE-DEPENDENCE OF A HOLOGRAPHIC BARYON

As mentioned above, by using the Witten Ansatz, $1+4$ dimensional holographic QCD is reduced into a $1+2$ dimensional Abelian Higgs theory. Accordingly, the topological description of a baryon is changed from an instanton to a vortex. In the previous section, we have numerically obtained the ground-state solution in holographic QCD, where the baryon size is automatically determined by minimizing the total energy.

Now, let us consider a holographic baryon with various size. Note that the size is originally one of the moduli of an instanton in a flat space, and different size baryons are to be degenerate in holographic QCD, if one sets $h(w)=k(w)=1$ and neglects the CS term. In the real holographic QCD, the size parameter is no more modulus, according to the background gravity and CS term. Nevertheless, the size might behave as a quasimodulus in the holographic baryon, resulting in physical appearance of a soft vibrational mode as a low-lying excitation. Then, we investigate a baryon with various size and size dependence of the energy in holographic QCD in this section.

First, we consider the ordinary Yang-Mills theory and examine the moduli relation between an instanton and a vortex in the Witten Ansatz, as was originally shown by Witten [37].

Next, we proceed to the holographic baryon, and consider how to obtain an arbitrary-size baryon as a solution of holographic QCD, and investigate the size dependence of the baryon mass.

A. Instanton-vortex correspondence in Yang-Mills theory

In the four-dimensional Euclidean Yang-Mills theory, there exist topological solutions, instantons, where Euclidean time is necessary. A single instanton solution (BPST-'t Hooft solution [35,36]) is written as

$$A_\mu(x)=-\eta^a_{\mu\nu}\tau^a\frac{x^\nu}{(x-X)^2+R^2},\tag{47}$$

where the instanton center locates at $x^\mu=X^\mu$, and R denotes the instanton size. Together with color rotation, the location X^μ and the size R are known as moduli, and they represent degrees of freedom for this topological solution, that is, their values do not affect the Yang-Mills action. Here, $\eta^a_{\mu\nu}$ denotes the 't Hooft symbol [36] defined by

$$\eta^a_{\mu\nu}=-\eta^a_{\nu\mu}=\begin{cases}\epsilon_{a\mu\nu} & \text{for } \mu,\nu=1,2,3\\ -\delta_{a\nu} & \text{for } \mu=4\\ \delta_{a\mu} & \text{for } \nu=4.\end{cases}\tag{48}$$

Taking its center $X^\mu=(\vec{0},T)$, there is SO(3) rotational symmetry in (x,y,z)-space, and the Witten Ansatz is applicable. With the Witten Ansatz, the four-dimensional Yang-Mills theory is reduced into a two-dimensional Abelian Higgs theory, and this instanton can be described by a single vortex.

To understand the relation between an instanton and a vortex, let us consider the 't Hooft solution in the form of the Witten Ansatz. This represents a single instanton solution and is rewritten as

$$A^a_i=\frac{2r}{r^2+(t-T)^2+R^2}\epsilon_{iaj}\hat{x}_j-\frac{2(t-T)}{r^2+(t-T)^2+R^2}(\hat{\delta}_{ia}+\hat{x}_i\hat{x}_a),\tag{49}$$

$$A^a_t=\frac{2r}{r^2+(t-T)^2+R^2}\hat{x}_a.\tag{50}$$

By comparing the functional form with Eqs. (5) and (6), SU(2) gauge fields can be converted into the fields of the reduced Abelian Higgs theory, and their forms are obtained as

$$(\phi_1,\phi_2+1)=\frac{2r}{r^2+(t-T)^2+R^2}(-(t-T),r),\tag{51}$$

$$a_1=\frac{-2(t-T)}{r^2+(t-T)^2+R^2},\quad a_2=\frac{2r}{r^2+(t-T)^2+R^2}.\tag{52}$$

The complex Higgs field $\phi = (\mathrm{Re}\phi, \mathrm{Im}\phi) = (\phi_1, \phi_2)$ takes zero at $(r, t) = (R, T) \equiv \zeta$. The vortex number is counted as the zero-point number in the Higgs field ϕ in the (r, t)-plane. Now, there is one zero point at ζ, and this configuration represents a single vortex.

Thus, in the Witten Ansatz, the vortex corresponding to a single instanton has a zero point ζ of the Higgs field ϕ. Remarkably, this Higgs-field zero point ζ relates to instanton parameters [37],

$$\zeta = (\zeta_r, \zeta_t) = (R, T). \tag{53}$$

In fact, the instanton size R and Euclidean fourth-coordinate T of the instanton center correspond to this zero point ζ in the Higgs field ϕ. In this configuration, the topological density is written by

$$\rho_B = \frac{6}{\pi^2} \frac{R^4}{[r^2 + (t-T)^2 + R^2]^4}. \tag{54}$$

The topological density localizes around $(r, t) = (0, T)$, and its extension is about the size parameter R, which reflects the instanton size.

B. Various-size baryon mass in holographic QCD

In this subsection, using the above correspondence (53) between the Higgs zero-point ζ and the instanton size R in the Witten Ansatz, we try to control the baryon size by changing the location of the zero point ζ in the Higgs field ϕ in holographic QCD. Using this new viewpoint, we obtain various sizes of holographic baryons and investigate size dependence of the single baryon energy.

To begin with, we reformulate the above argument for $1+4$ dimensional holographic QCD. We recall different points from the ordinary Yang-Mills theory. First, holographic QCD already has four-dimensional Euclidean space of (x, y, z, w), and the instanton can be naturally defined on this space including the fourth spatial coordinate w, without use of Euclidean process. Second, there appear the gravitational factor, $h(w)$ and $k(w)$, and the CS term, which results in a repulsive interaction among the baryon density ρ_B in holographic QCD. Owing to these effects, the 't Hooft solution is no longer the exact solution but an approximate one in holographic QCD.

Therefore, we use the 't Hooft solution as a starting point for the $B = 1$ configuration, and search for the true solution of holographic QCD by a numerical iterative method with keeping the topological property unchanged, similarly in Sec. IV.

In $1+4$ dimensional holographic QCD, taking the $A_0 = 0$ gauge, we use a holographic version of the 't Hooft solution (47), as a starting point of the topological configuration. Here, we locate the instanton center at the four-dimensional spatial origin $(x, y, z, w) = (0, 0, 0, 0)$ for symmetry of (x, y, z)-spatial rotation and w-reflection, and then the initial configuration is set to be

$$A_0 = 0, \tag{55}$$

$$A_M = -\eta_{MN} \frac{x^N}{x^2 + R^2}, \tag{56}$$

which can be rewritten as

$$A_i^a = \frac{2r}{r^2 + w^2 + R^2} \epsilon_{iaj} \hat{x}_j - \frac{2w}{r^2 + w^2 + R^2} (\hat{\delta}_{ia} + \hat{x}_i \hat{x}_a), \tag{57}$$

$$A_w^a = \frac{2r}{r^2 + w^2 + R^2} \hat{x}_a. \tag{58}$$

For the (x, y, z)-rotational symmetric system, through the Witten Ansatz, the non-Abelian gauge fields are converted into the Higgs field ϕ and Abelian gauge field $\vec{a}$, and they are expressed as

$$(\phi_1, \phi_2 + 1) = \frac{2r}{r^2 + w^2 + R^2} (-w, r), \tag{59}$$

$$a_1 = \frac{-2w}{r^2 + w^2 + R^2}, \qquad a_2 = \frac{2r}{r^2 + w^2 + R^2}. \tag{60}$$

In Eq. (59), the zero point ζ of the Higgs field ϕ is found to locate at $\zeta = (\zeta_r, \zeta_w) = (R, 0)$, and this ζ_r determines the initial size of the holographic baryon.

From this initial configuration, similarly in Sec. IV, we numerically search for the single baryon solution in holographic QCD by minimizing the total energy $E[\phi, \vec{a}, \hat{A}_0]$, with fixing the Higgs-zero location

$$\zeta = (\zeta_r, \zeta_w) = (R, 0), \tag{61}$$

where the former R corresponds to the instanton/baryon size. In fact, to consider various size baryons, we here use the correspondence between the instanton/baryon size and zero point ζ in the Higgs field ϕ composing the Abrikosov vortex [37]. Note that the Higgs field must be zero at the center of the Abrikosov vortex to realize the finite energy, and therefore the Higgs field ϕ inevitably has a zero-point ζ in the presence of the vortex corresponding to $B = 1$ in holographic QCD. Here, to change the zero-point location $\zeta_r = R$ corresponds to a baryon-size change, and its various changes lead to different-size baryons.

In summary, to obtain various-size baryon solutions, we fix this zero-point location $\zeta = (\zeta_r, \zeta_w) = (R, 0)$ of the Higgs field ϕ as a boundary condition and minimize the total energy E numerically. When the total energy $E[\phi, \vec{a}, \hat{A}_0]$ is minimized against arbitrary local variation of

ϕ, $\vec{a}$ and $\hat{A}_0$, these fields satisfies the EOM of holographic QCD.

For the numerical calculation on the (r, w) plane, we use the same lattice used in Sec. IV, that is, a fine and large-size lattice with spacing of $0.2\ M_{\rm KK}^{-1} \simeq 0.04$ fm and the extension of $0 \leq r \leq 250$ and $-125 \leq w \leq 125$, of which physical size is $(50\ M_{\rm KK}^{-1})^2 \simeq (10\ {\rm fm})^2$.

After an iterative improvement of holographic fields with the constraint of the Higgs zero-point location, we eventually obtain the Higgs and Abelian gauge fields,

$$\phi(r, w; R), \qquad \vec{a}(r, w; R), \qquad \hat{A}_0(r, w; R) \tag{62}$$

for the holographic baryon corresponding to the instanton size R. Note again that the presence of a zero point of the Higgs field indicates a $B = 1$ configuration, and the holographic fields obeying the local energy minimum condition also satisfy the EOM of holographic QCD.

Figure 7 shows the static energy $V(R)$ of the baryon with various size R. The potential minimum corresponds to the ground-state baryon. The numerical data are well fitted by a quadratic function, as shown in Fig. 7. Note that all the symbols represent the solution of holographic QCD under the constraint of size fixing, which can be regarded as a boundary condition.

We obtain the fitting quadratic function,

$$V(R) \simeq A(R - R_0)^2 + M_0, \qquad A \simeq 0.063, \qquad R_0 \simeq 2.4, \qquad M_0 \simeq 1.25, \tag{63}$$

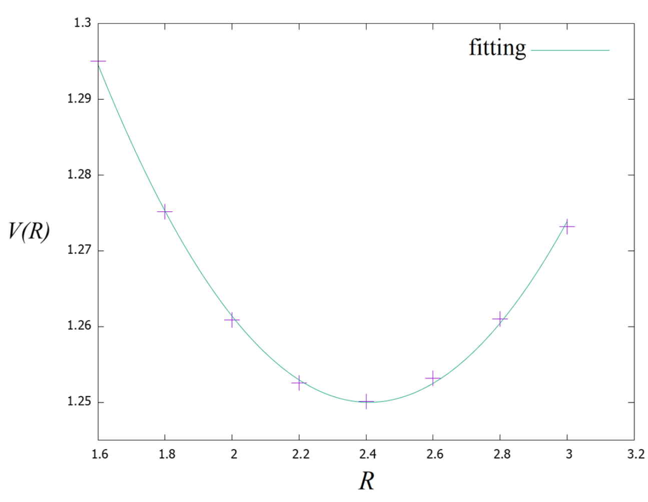

FIG. 7. Static energy $V(R)$ of the baryon with various size R in the $M_{\rm KK} = 1$ unit. The symbol denotes numerical data of the baryon energy with different sizes. The line denotes a fit curve of the potential by a quadratic function. This potential has a minimum corresponding to the ground-state, and its value is consistent with the previous ground-state calculation.

in the $M_{\rm Kk} = 1$ unit. The value M_0 of potential minimum coincides with the previous calculation of the ground-state baryon mass $M_B \simeq 1.25\ M_{\rm KK}$ in Eq. (39).

The size parameter $R = R_0$ which minimizes the static energy $V(R)$ of the baryon is found to be $R_0 \simeq 2.4$ in the $M_{\rm KK} = 1$ unit. This result coincides with the ground-state result shown in Fig. 1, where the Higgs zero-point ζ_r locates at about $R = R_0$. If there were no nontrivial gravity $[h(w), k(w)]$ and no CS term, this size dependence would disappear and the potential $V(R)$ would become flat because the instanton size is originally a modulus, reflecting classical scale invariance of the Yang-Mills theory. In fact, this size dependence of holographic baryon mass originates from those gravitational effects and CS term.

C. Analysis of holographic baryon size

In this subsection, we investigate actual size of holographic baryons obtained in the previous subsection in terms of the size parameter R, which corresponds to the instanton size.

In our calculation, for each constraint of fixing the size R, we already obtain the topological density ρ_B as

$$\rho_B = \rho_B(r, w; R). \tag{64}$$

Using this gauge-invariant local quantity, we investigate the size of the holographic baryon for each direction of r and w. Here, we define ρ_B-weighted average of arbitrary (x, y, z)-rotational symmetric variable $O(r, w)$ as

$$\langle O \rangle_{\rho_B(R)} \equiv \frac{\int_0^\infty dr r^2 \int_{-\infty}^\infty dw \rho_B(r, w; R) O(r, w)}{\int_0^\infty dr r^2 \int_{-\infty}^\infty dw \rho_B(r, w; R)}. \tag{65}$$

In the ordinary four-dimensional Euclidean Yang-Mills theory, the Pontryagin density ρ of a single instanton with the size parameter R and its center at the origin is given by

$$\rho = \frac{1}{16\pi^2} {\rm tr}(F_{\mu\nu} \tilde{F}_{\mu\nu}) = \frac{6}{\pi^2} \frac{R^4}{(x_\mu^2 + R^2)^4}, \tag{66}$$

and the mean square radius weighted with ρ is evaluated as

$$\langle r^2 \rangle_\rho = \frac{3}{2} R^2, \qquad \langle t^2 \rangle_\rho = \frac{1}{2} R^2 \quad \text{(YM instanton)}, \tag{67}$$

or equivalently

$$\sqrt{\frac{2}{3} \langle r^2 \rangle_\rho} = \sqrt{2 \langle t^2 \rangle_\rho} = R \quad \text{(YM instanton)}, \tag{68}$$

for $r \equiv (x^2 + y^2 + z^2)^{1/2}$ and the Euclidean time t.

The holographic baryon is able to be dilatated simultaneously in both r and w direction, imposing the Higgs field zero-point constraints, and we obtain various size baryons. Based on the above relation, we consider size parameters of the holographic baryon in r and w directions, respectively. In a similar manner to Eq. (40) in Sec. IV, we define the radius weighted with the topological density ρ_B as

$$d_r(R) \equiv \sqrt{\frac{2}{3}\langle r^2\rangle_{\rho_B(R)}}, \qquad d_w(R) \equiv \sqrt{2\langle w^2\rangle_{\rho_B(R)}}, \qquad (69)$$

in the direction r and w, respectively. To compare with the instanton size parameter R, the factors, $2/3$ and 2, have been introduced, considering Eq. (68). In fact, the ordinary self-dual Yang-Mills instanton satisfies $d_r(R) = d_w(R) = R$.

Figure 8 shows the ρ_B-weighted radius $d_r(R)$ and $d_w(R)$ as a function of R, weighted with the topological density.

The solid line denotes $d = R$ and is realized in the case of the ordinary four-dimensional YM theory ($h(w) = k(w) = 1$) without the CS term. In other words, if the holographic baryon were described with the 't Hooft solution, one would find $d_r(R) = d_w(R) = R$.

From Fig. 8, d_r and d_w are found to be monotonically increasing along with R. This monotonical increase reflects that the change of Higgs zero-point gives the change of holographic baryon (instanton) size. Later, we investigate the dilatation mode by regarding the size R as dynamical degree of freedom.

Around the ground state ($R = R_0 \simeq 2.4$), the value of $d_r(R)$ is larger than $d_w(R)$, i.e., $d_r(R) > d_w(R)$, and this means an oblate-shaped instanton for the holographic baryon [24].

The slope of $d_r(R)$ is larger than $d_w(R)$, and $d_w(R)$ is almost flat against R. Therefore, the size change of holographic baryons is approximately regarded as three-dimensional in r-direction rather than four-dimensional. (See Appendix C and D for four-dimensional size change using the BPS instanton.)

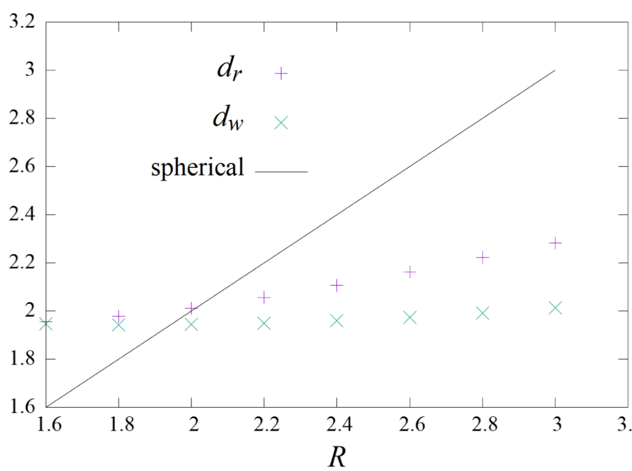

FIG. 8. ρ_B-weighted radius $d_r(R)$ and $d_w(R)$ of the holographic baryon in the direction r and w, respectively, as the function of the size parameter R in the $M_{KK} = 1$ unit. The solid line denotes $d = R$, which is to be realized in the case of the ordinary four-dimensional YM theory ($h(w) = k(w) = 1$) without the CS term. If the holographic baryon were described with the 't Hooft solution, $d_r(R) = d_w(R) = R$ would be satisfied.

These differences of the behavior for each direction would come from the nontrivial gravity fields, $h(w)$ and $k(w)$, because the CS term (23) equally acts in r and w-direction and does not break (x, y, z, w) $O(4)$ symmetry. In fact, if $h(w) = k(w) = 1$, $O(4)$ symmetry is exact and no (r, w)-asymmetry appears. Therefore, $h(w)$ and $k(w)$ are the very origin of (r, w)-asymmetry.

The flatness of $d_w(R)$ against R indicates that gravity fields $h(w)$ and $k(w)$ suppress the w-direction swelling. Approximately, one finds $d_r(R) \sim d_w(R)$, and then $d_r(R)$ seems to follow $d_w(R)$ and its soft R-dependence, which might imply that large deviation from the spherical shape is not favored energetically. As the result, the slope of both parameters become small.

In the original Yang-Mills theory, the (anti)instanton appears as the (anti)self-dual solution. In holographic QCD, owing to the presence of gravity [$h(w)$ and $k(w)$] and the CS term, the self-duality of the solution is explicitly broken.

Similarly for the ground-state baryon in Sec. IV, we investigate self-duality breaking for various size holographic baryons. Figure 9 shows the self-duality breaking parameter Δ_{DB} in Eq. (46) as a function of the size parameter R. This quantity Δ_{DB} is non-negative and becomes zero only in the exact self-dual case.

One finds that the duality breaking parameter is minimized as $\Delta_{\mathrm{DB}} \simeq 0.17$ at $R \simeq 2.2$, which is close to the size $R_0 \simeq 2.4$ of the ground-state baryon. This value $\Delta_{\mathrm{DB}} \simeq 0.17$ seems to be small, and one might expect that the approximation of using the self-dual solution is not so bad.

However, the duality breaking parameter Δ_{DB} never becomes zero in holographic QCD, and this fact might have an important physical meaning for the baryon-baryon interaction as follows.

In the original four-dimensional Yang-Mills theory, the energy is classically bounded by BPS bound, and its

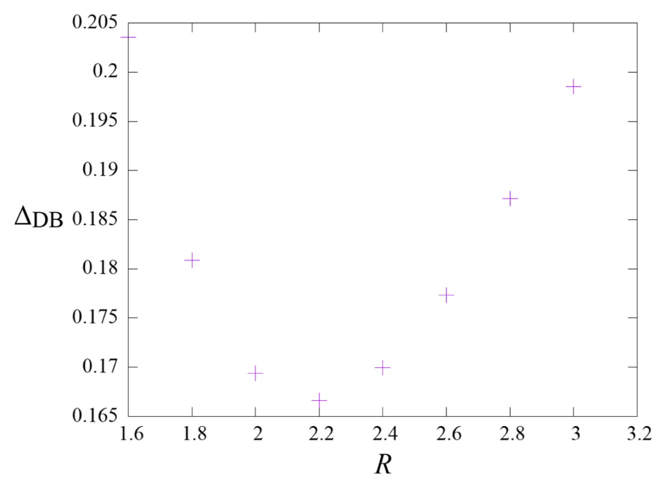

FIG. 9. Duality breaking parameter Δ_{DB} for various baryon size R in the $M_{KK} = 1$ unit. The functional form of $\Delta_{\mathrm{DB}}(R)$ seems to be quadratic and it takes minimum at $R \simeq 2.2$.

minimum is achieved only if the configuration has self-duality. However, holographic QCD has a nontrivial gravity and the CS term, and thus they distort the self-duality. If there were multi instantons satisfying BPS saturation, its action would be determined only by the topological charge, indicating the “no interaction” between instantons. Then, as an interesting possibility, the self-duality breaking in holographic QCD might be related to the baryon-baryon interaction or the nuclear force [38].

VI. DILATATION MODE OF A SINGLE BARYON

In the previous section, we investigated size dependence of the static energy $V(R)$ of a holographic baryon and showed that it seemed to be quadratic against the size R. Using this result, we numerically investigate time-dependent size oscillation modes, i.e., dilatation modes, of a single baryon in holographic QCD in this section.

Since the instanton size R is a key parameter to determine the baryon size in holographic QCD, we describe the size oscillation of the holographic baryon by introducing time-dependence of size R,

$$R \to R(t) = R_0 + \delta R(t), \tag{70}$$

where R_0 denotes the size of the ground-state baryon and the size $R(t)$ is expected to oscillate around this R_0.

Note again that the size of an instanton is originally a moduli, and, if there were only the Yang-Mills term in flat space $h(w) = k(w) = 1$, its value would not affect the energy of holographic QCD and the dilatation mode would appear as an exact zero mode. In reality, the gravity effect $[h(w), k(w)]$ and CS term break this moduli property of the size; however, we expect that the dilatation mode is inherited to be a soft mode of the ground-state baryon and appears as a low-lying excitation in the single baryon spectrum in holographic QCD. As a characteristic property, the dilatation never changes the flavor and rotational properties and hence the dilatation excitation has the same quantum number as the ground state.

This dilatation differs from an ordinary (x, y, z)-spatial size oscillation, because holographic QCD has an extra dimension w and the holographic baryon extends also its direction. In fact, this extra-dimensional dilatation is peculiar to holographic QCD.

We consider time-dependent variation of $R(t)$ around the ground-state size R_0, which physically means a dilataion of the holographic baryon. The Lagrangian of the size variable $R(t)$ is written as

$$\begin{aligned} L[R] &= \frac{1}{2} m_R \dot{R}^2 - V(R) \\ &\simeq \frac{1}{2} m_R \dot{R}^2 - \frac{1}{2} m_R \omega^2 (R - R_0)^2 \end{aligned} \tag{71}$$

up to $\mathcal{O}((R - R_0)^2)$. We have already calculated the potential term $V(R)$ and have shown it to be almost quadratic in the previous section.

We calculate the dilatation mode of the holographic baryon as a collective coordinate motion of the size $R(t)$. Note here that, to estimate the frequency ω of the dilatational mode, one only has to calculate the mass parameter m_R. (Of course, m_R is not equal to the baryon mass M_B.) Here, we use adiabatic approximation that time-dependence of the holographic fields is only through the size $R(t)$.

A. Numerical calculation

In this subsection, we consider the baryon dilatation mode and investigate the excitation energy with keeping the gravity background, $h(w)$ and $k(w)$. We treat the size oscillation to be adiabatic and field motions are relatively faster than the size motion. Within this adiabatic treatment, the time dependence of holographic fields ϕ and a_i is decided through only the baryon size $R(t)$. Therefore, it is possible to write down field arguments symbolically as

$$\phi = \phi(r, w; R(t)), \qquad a_i = a_i(r, w; R(t)). \tag{72}$$

Note that there is no contribution from $\hat{A}_0$ in calculating the kinetic term of size variable $R(t)$, because $\hat{A}_0$ has no time-derivative and never accompanies $\dot{R}(t)$.

Based on this adiabatic treatment, time-derivative is converted to R-derivative as

$$\frac{d}{dt} O[R(t)] = \dot{R} \frac{d}{dR} O[R]. \tag{73}$$

In our framework, $O[R]$ is (numerically) calculable for arbitrary R, and the R-derivative is easily obtained numerically,

$$\frac{d}{dR} O[R] \simeq \frac{O[R + \delta R] - O[R]}{\delta R}. \tag{74}$$

We have already obtained holographic configurations $\phi(R(t))$ with various size R, and the kinetic term of $R(t)$ is expressed as

$$\begin{aligned} S_{\mathrm{kin}} &= 4\pi\kappa \int dt \int_0^\infty dr \int_{-\infty}^\infty dw \\ &\quad \times \left[h|\partial_0 \phi|^2 + h\frac{r^2}{2} (\partial_0 a_1)^2 + k\frac{r^2}{2} (\partial_0 a_2)^2 \right] \\ &= 4\pi\kappa \int dt \int_0^\infty dr \int_{-\infty}^\infty dw \\ &\quad \times \left[h\dot{R}^2 |\partial_R \phi|^2 + h\frac{r^2}{2} \dot{R}^2 (\partial_R a_1)^2 + k\frac{r^2}{2} \dot{R}^2 (\partial_R a_2)^2 \right] \\ &= \int dt \frac{1}{2} m_R \dot{R}^2, \end{aligned} \tag{75}$$

and mass parameter m_R on the size variation is given by

$$m_R \equiv 8\pi\kappa \int_0^\infty dr \int_{-\infty}^\infty dw \times \left[h|\partial_R \phi|^2 + h\frac{r^2}{2}(\partial_R a_1)^2 + k\frac{r^2}{2}(\partial_R a_2)^2\right]. \quad (76)$$

Note that CS term also contains time derivative, but it is first order and no effect from the CS term for the kinetic term of dilatation mode. The numerical result is found to be

$$m_R \simeq 0.34\ M_{\rm KK} \simeq 322\ \text{MeV}. \quad (77)$$

The important point of this numerical calculation is that gravitational factors, $h(w)$ and $k(w)$, are exactly included.

With this value of the mass parameter m_R and the quadratic fitting of Eq. (63) for the potential $V(R)$, we obtain the dilatational excitation energy

$$\omega = \sqrt{\frac{2A}{m_R}} \simeq 0.61\ M_{\rm KK} \simeq 577\ \text{MeV} \quad (78)$$

for the holographic baryon.

In terms of $1/N_c$ expansion, the mass parameter $m_R \propto \kappa$ in Eq. (78) is $O(N_c)$, and the potential $V(R)$ of the holographic baryon is $O(N_c)$, leading to $A = O(N_c)$. Then, the dilatation excitation energy $\omega = \sqrt{2A/m_R}$ is $O(N_c^0) = O(1)$ quantity.

In Appendix D, we also consider a rough analytical estimation for the dilatation mode, when using 't Hooft instanton, i.e., the solution in the case of $h(w) = k(w) = 1$ without the CS term. This rough estimate gives a larger value of 771 MeV for the dilatation excitation energy, which seems consistent with $0.816\ M_{\rm KK} \simeq 774$ MeV of the excitation energy on instanton-size fluctuation in the previous research [19] using 't Hooft instanton.

B. Discussion

In the previous subsection, we numerically calculate the dilatation excitation energy, keeping the gravitational effect of $h(w)$ and $k(w)$. Note again that this background gravity is physically important because it is inherited from the N_c D4 branes to express the original Yang-Mills theory. We have consistently performed a numerical calculation for both kinetic and potential terms to include the gravitational effect. We have eventually obtained the dilatation excitation energy of 577 MeV for the holographic baryon.

This dilatation mode appears as an excited baryon with the same quantum number as the ground state since this rotationally symmetric dilatation never changes the quantum numbers on the flavor and rotation.

Similar to the Skyrme soliton, for the description of definite spin/isospin states like N and Δ, semi-classical quantization by adiabatic rotation [19] is used for the holographic baryon. In this quantization process on the spin/isosipn, an $O(1/N_c)$ mass correction is added to the $O(N_c)$ baryon mass [19].

In terms of $1/N_c$ expansion, the dilatation excitation energy is $O(N_c^0)$ as mentioned before, and thus the dilatation mode is more significant than the $O(1/N_c)$ rotational energy, which leads to N-Δ mass splitting. Furthermore, the correction from this rotational effect to the dilatation mode is higher order of $1/N_c$ expansion and then becomes negligible.

Figure 10 shows schematic figure for the baryon mass splitting order by order in the $1/N_c$ expansion. At the leading order of $O(N_c)$, all the holographic baryons degenerate. Up tp $O(N_c^0)$, there appears the mass splitting of dilatation mode. Up to $O(N_c^{-1})$, the mass splitting from rotational effect is added and leads to N-Δ mass splitting. As the result, the order of low-lying baryon mass is to be $\mathrm{N} < \Delta < \mathrm{N}^* < \Delta^*$ in term of the $1/N_c$ expansion.

In holographic QCD, the dilatation excitation seems to appear as the first excitation of the ground-state baryon and has the same quantum number, e.g., positive parity. In addition to the qualitative properties, the dilatation excitation energy is estimated as 577 MeV in holographic QCD. From these results on the same quantum number and the magnitude of the excitation energy, this dilatation mode of the nucleon N(940) would be identified as the Roper resonance N*(1440), which is positive parity and the first excitation of N(940). For the Δ(1232), Δ(1600) might be identified to be the dilatational excitation mode.

As an interesting possibility, the similar dilatation mode exists for every baryon as a universal phenomenon for a single baryon, because any extended stable soliton generally has such a dilatational mode.

The strange baryon mass is slightly larger, reflecting the non-zero strange quark mass; however, the $SU(3)_f$ flavor symmetry approximately holds. Here, we suppose that the mass excess of the strange quark is simply added to the holographic baryon, like the treatment of $SU(3)_f$ symmetry and its breaking in ordinary hadron physics [39]. Then, also for strange baryons, the dilatation mode would appear, and

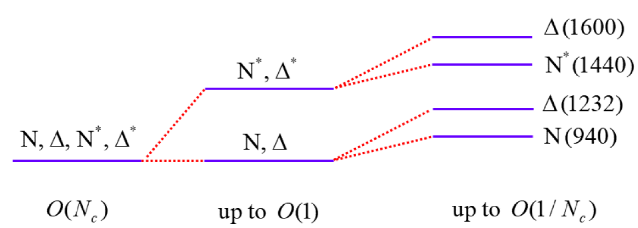

FIG. 10. Schematic figure for mass splitting of the holographic baryon in terms of the $1/N_c$ expansion. (The symbol * denotes the excitation mode.) The holographic baryon has $O(N_c^0)$ and $O(N_c^{-1})$ splitting, corresponding to dilatation and rotational effect, respectively. Therefore, the order of low-lying baryon mass is to be $\mathrm{N} < \Delta < \mathrm{N}^* < \Delta^*$ in term of the $1/N_c$ expansion.

TABLE I. Experimental candidates of the dilatational excitation mode in various baryon channel [40]. Each ground-state baryon has the excitation with the same quantum number. Here, first-excited baryons are mainly listed, such as $N^*(1440)$ and $\Delta(1600)$. For each channel, the excitation energy seems to take a consistent value with the theoretical one, $\omega \simeq 577$ MeV. Here, $N^*(1710)$ and $\Delta(1920)$ are identified to the second excitation mode.

Baryon	Excited baryon	Excitation energy	Theory
N(940)	$N^*(1440)$	500 MeV	ω
	$N^*(1710)$	770 MeV	2ω
$\Delta(1232)$	$\Delta(1600)$	368 MeV	ω
	$\Delta(1920)$	688 MeV	2ω
$\Lambda(1116)$	$\Lambda(1600)$	484 MeV	ω
$\Sigma(1193)$	$\Sigma(1660)$	467 MeV	ω
$\Sigma^*(1385)$	$\Sigma^*(1780)$	395 MeV	ω

its excitation energy is expected to take a similar value as the above result of 577 MeV.

Table I presents the candidates of the dilational excitation in various channel of baryons, i.e., N, Δ and Λ, Σ, Σ^* channel.

For each channel with the same quantum number, we find that the first excitation energy seems to be a consistent similar value to the dilatational one, $\omega \simeq 577$ MeV, theoretically obtained above.

Also for multi-strange baryons in Ξ, Ξ^* and Ω channel, we theoretically predict the dilatation modes with the excitation energy of about 577 MeV. However, the dilatational excited baryons for $\Xi(1320)$, $\Xi^*(1530)$, and $\Omega(1673)$ are not yet observed experimentally because spin-parity information is not yet confirmed for their excited baryons. In this respect, further experimental analyses are much desired for excited baryons in terms of the dilatational mode in each baryon channel.

VII. SUMMARY AND CONCLUDING REMARKS

We have investigated a baryon and its dilatation modes in holographic QCD based on the Sakai-Sugimoto model, which is constructed with N_c D4 branes and N_f D8/$\overline{\text{D8}}$ branes in the superstring theory. This theory is expressed as a $1+4$ dimensional $\mathrm{U}(N_f)$ gauge theory in the flavor space.

We have adopted a generalized version of the Witten Ansatz for spatially rotational symmetric systems and have reduced $1+4$ dimensional holographic QCD into a $1+2$ dimensional Abelian Higgs theory in a curved space. In this formulation, a four-dimensional instanton corresponding to a baryon is converted to a two-dimensional Abrikosov vortex. We have numerically calculated the baryon solution of holographic QCD using a fine and large-size lattice with spacing of 0.04 fm and size of 10 fm.

Using the relation between the baryon size and the zero-point location of the Higgs field in the Witten Ansatz, we have theoretically changed the size of holographic baryons and have investigated its properties, such as the energy and self-duality breaking, as function of the size parameter. Here, each configuration is a solution of EOM of holographic QCD under the constraint of fixing Higgs zero-point.

As time-dependent size-oscillation modes, we have investigated the dilatation modes of a baryon and have found that such a dilatational mode takes the excitation energy of 577 MeV. Since the dilatation does not change the quantum number including the parity, we have identified this dilatation mode for the nucleon N(940) as the Roper resonance $N^*(1440)$. We have conjectured that any baryons are expected to have such a dilatational excitation universally, and their excitation energy would be similar.

In this respect, further experimental analyses are much desired for excited baryons in terms of the dilatational mode in each baryon channel. In particular, the dilatational excited baryons for $\Xi(1320)$, $\Xi^*(1530)$, and $\Omega(1673)$ have not yet been observed experimentally because spin-parity information is not yet confirmed for their excited baryons.

As a caution, the calculated values presented in this paper are to be regarded as semiquantitative estimates in an idealized case of large N_c in the chiral limit, and they have some deviation from experimental values in the real world. In the following, we mention some quantitative limitations and cautions on the approach used in this study.

This framework of holographic QCD has infrared equivalence with massless QCD and gives a useful analytical nonperturbative method to analyze QCD, which is a main reason to adopt holographic QCD in this study for baryons. On the quantitative accuracy, however, this framework includes some limitations. As an important caution, the present calculation is based on the $1/N_c$ and $1/\lambda$ expansion, and the starting holographic action is up to the $1/N_c$-leading and $1/\lambda$ sub-leading order. Therefore, for more accurate estimation, it is desirable to check the contribution from $1/N_c$ or $1/\lambda$ higher order terms. However, it is extremely difficult to extract the next order of $1/N_c$ and $1/\lambda$ expansions in holographic QCD.

As a higher-order correction, there is an $O(1/N_c)$ rotational effect of the hedgehog configuration, which is used for semi-classical analysis of the Skyrmion investigation [41]. It is relatively $1/N_c^2$ smaller, compared with leading order $O(N_c)$ of the baryon mass, although it is necessary for the N-Δ splitting. Similarly, for the dilatational excitation, this correction appears as relatively $1/N_c^2$-smaller order, and therefore we have ignored this higher order in this paper. However, this higher-order correction might be desired to reproduce real experimental data.

In addition, we have assumed spatially spherical shape of a baryon to apply the Witten Ansatz and adiabatic treatment for the dilatation dynamics. For more precise analysis of baryons, more sophisticated treatments might be desired. However, to go beyond the spherical symmetric solution, the Witten Ansatz is no more applicable, and then one has to deal with the four-dimensional analysis even for static baryons. To go beyond adiabatic approach is also a difficult problem widely appeared in theoretical physics, and one has to handle complicated local oscillation of all the holographic fields in the present case.

We have used holographic QCD based on $N_f = 2$ in the chiral limit. Further extension including strangeness is an interesting subject in hadron physics, which can be done with $N_f = 3$ holographic QCD [42]. In the real world, u and d-quarks have small finite current mass of 2–5 MeV and s-quarks have current mass of about 93 MeV [40], and the non-zero quark mass explicitly breaks the chiral symmetry. In holographic QCD, however, it is difficult to introduce the finite quark mass or explicit chiral-symmetry breaking, and further theoretical development is required for quantitative argument of hyperons.

We have mainly presented the excitation energy for the dilatational mode of baryons, which appears in the same quantum numbers. It is desired for theoretical progress to show how to distinguish the dilatational mode from other excitation experimentally. To this end, we have to find out unique behavior for the dilatational mode, which is a future subject. The finding of such a peculiar quantity will lead to a better understanding of baryon spectra.

ACKNOWLEDGMENTS

H. S. is supported in part by the Grants-in-Aid for Scientific Research [19K03869] from Japan Society for the Promotion of Science.

APPENDIX A: LATTICE FORMALISM OF HOLOGRAPHIC QCD

In Appendix A, we show our lattice formalism for holographic QCD in the Witten Ansatz, by introducing a sizable finite lattice with a small spacing a.

Let us begin with the static energy $E_{5\mathrm{YM}}$ of the Yang-Mills term in the Witten Ansatz. For the explanation, we here repeat Eq. (18),

$$E_{5\mathrm{YM}} = 4\pi\kappa \int_0^\infty dr \int_{-\infty}^\infty dw \left[h(w)|D_1\phi|^2 + k(w)|D_2\phi|^2 + \frac{h(w)}{2r^2}\{1-|\phi|^2\}^2 + \frac{r^2}{2}k(w)f_{12}^2 \right], \tag{A1}$$

of which the field variables ϕ and a_μ depend on the two-dimensional spatial coordinate (r, w).

For the U(1) gauge variable a_μ with $\mu = r, w$, we define the link variable

$$U_\mu(s) \equiv \exp\left\{ i a a_\mu \left(s + \frac{\hat{\mu}}{2} \right) \right\} \in \mathrm{U}(1) \tag{A2}$$

at the site $s = (s_r, s_w)$ on the two-dimensional lattice. Here, $\hat{\mu}$ denotes the μ-directed vector with the length of a.

On the lattice with a small spacing a, one finds for the U(1) covariant derivative $D_\mu\phi$ as

$$\begin{aligned}
&-\{\phi^\dagger(s)U_\mu(s)\phi(s+\hat{\mu}) + \phi^\dagger(s+\hat{\mu})U_\mu(s)^\dagger\phi(s)\} + |\phi(s)|^2 + |\phi(s+\hat{\mu})|^2 \\
&= -\left(\phi - \frac{a}{2}\partial_\mu\phi\right)^\dagger \left(1 + iaa_\mu - \frac{1}{2}a^2a_\mu^2\right)\left(\phi + \frac{a}{2}\partial_\mu\phi\right) - \left(\phi + \frac{a}{2}\partial_\mu\phi\right)^\dagger \left(1 - iaa_\mu - \frac{1}{2}l^2a_\mu^2\right)\left(\phi - \frac{a}{2}\partial_\mu\phi\right) \\
&\quad + 2|\phi|^2 + \frac{a^2}{2}|\partial_\mu\phi|^2 + \mathcal{O}(a^3) \\
&= a^2\phi^\dagger(\overleftarrow{\partial_\mu} - ia_\mu)(\partial_\mu + ia_\mu)\phi + \mathcal{O}(a^3) \\
&= a^2|D_\mu\phi|^2 + \mathcal{O}(a^3),
\end{aligned} \tag{A3}$$

where all omitted arguments are $s + \hat{\mu}/2$. The field strength f_{12} is expressed with the U(1) plaquette variable,

$$\square_{12}(s) \equiv U_1(s)U_2(s+\hat{1})U_1^*(s+\hat{2})U_2^*(s) \in \mathrm{U}(1) \tag{A4}$$

$$f_{12}^2(s) = \frac{1}{a^2}[1 - \mathrm{Re}\{\square_{12}(s)\}]. \tag{A5}$$

The additional U(1) energy $E^{\mathrm{U}(1)}$ in Eq. (28) is expressed by the coupling of the original U(1) gauge field $\hat{A}_0$ and the topological density ρ_B. Here, the temporal component $\hat{A}_0(r, w)$ is treated as a (spatially) site-variable on the (r, w) lattice. On the lattice, the baryon density is expressed as

$$\begin{aligned}
\rho_B &= \frac{1}{8\pi^2r^2}[-i\epsilon_{ij}(D_i\phi)^*D_j\phi + \epsilon_{ij}\partial_i a_j(1-|\phi|^2)] \\
&= \frac{1}{8\pi^2r^2}[2\mathrm{Im}\{(D_1\phi)^*D_2\phi\} + f_{12}(1-|\phi|^2)]
\end{aligned} \tag{A6}$$

with

$$f_{12}(1-|\phi|^2) = \frac{1}{a^2}\mathrm{Im}\square_{12} \times (1-|\phi|^2) \tag{A7}$$

and

$$
\begin{aligned}
(D_1\phi)^* D_2\phi &= \frac{1}{4a^2}\{U_1^*(s)\phi^*(s+\hat{1}) - U_1(s-\hat{1})\phi^*(s-\hat{1})\}\{U_2(s)\phi(s+\hat{2}) - U_2^*(s-\hat{2})\phi(s-\hat{2})\} \\
&= \frac{1}{4a^2}\{\phi^*(s+\hat{1})U_1^*(s)U_2(s)\phi(s+\hat{2}) - \phi^*(s-\hat{1})U_1(s-\hat{1})U_2(s)\phi(s+\hat{2}) \\
&\quad - \phi^*(s+\hat{1})U_1^*(s)U_2^*(s-\hat{2})\phi(s-\hat{2}) + \phi^*(s-\hat{1})U_1(s-\hat{1})U_2^*(s-\hat{2})\phi(s-\hat{2})\}. \qquad \text{(A8)}
\end{aligned}
$$

To reduce the discretization error, we have used the above form for $(D_1\phi)^*D_2\phi$, and its lattice formalism is symbolically written as

$4a^2(D_1\phi)^*D_2\phi =$ 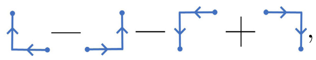 , (A9)

where the horizontal an vertical arrows represent U_1 and U_2, respectively, and the dots represent ϕ. Thus, we define the topological density $\rho_B(r,w)$ and formulate the U(1) energy $E^{\mathrm{U}(1)}[\rho_B(r,w),\hat{A}_0(r,w)]$ in Eq. (28) on the (r,w) lattice.

In this way, the total energy E in holographic QCD is expressed as $E[\phi(s),\vec{U}(s),\hat{A}_0(s)]$, i.e., a function of $\phi(s) = \phi_1(s) + i\phi_2(s) \in \mathbf{C}$, $\vec{U}(s) \equiv (U_1(s), U_2(s))$ and $\hat{A}_0(s)$ at the spatial site $s = (s_r, s_w)$. To find the solution of holographic QCD, we minimize the total energy E by iterative improvement on $\phi(s)$, $\vec{U}(s)$, and $\hat{A}_0(s)$. Looking at a specific site s_0, we consider only one variable $\phi(s_0)$, with fixing all other variables. By taking variation of $\phi(s_0)$, we minimize the total energy E. Next, we consider only one link-variable $\vec{U}(s_0)$, with fixing all other variables, and take its variation to minimize E. Similarly, considering only one site-variable $\hat{A}_0(s_0)$, with fixing all other variables, we take its variation to minimize E. On each site on the lattice, we repeat the above process and update $\phi(s)$, $\vec{U}(s)$ and $\hat{A}_0(s)$. We iterate this sweep procedure many times so as to minimize the total energy E in holographic QCD, and the solution is eventually obtained.

APPENDIX B: OTHER EXPRESSION OF U(1)-PART ENERGY

For the U(1) sector, we have mainly used Eq. (28) for the numerical calculation of $E^{\mathrm{U}(1)}$. However, there is another useful expression for the energy $E^{\mathrm{U}(1)}$ of the U(1) sector without $\hat{A}_0$, and we introduce this form in Appendix B.

By solving $\hat{A}_0$ using Eq. (25), the energy (27) becomes

$$
\begin{aligned}
E^{\mathrm{U}(1)} &= \frac{N_c^2}{8}\int d^3x dw \rho_B K^{-1}\rho_B \\
&= \frac{N_c^2}{8}\int d^3x dw \int d^3x' dw' \\
&\quad \times \rho_B(\vec{x},w)K^{-1}(\vec{x},w;\vec{x}',w')\rho_B(\vec{x}',w'). \qquad \text{(B1)}
\end{aligned}
$$

Since the kernel K and topological density ρ_B are SO(3) rotationally symmetric, the additional energy can be expressed only with the (r,w)-coordinates:

$$
\begin{aligned}
E^{\mathrm{U}(1)} &= 2\pi^2 N_c^2 \int_0^\infty dr \int_{-\infty}^\infty dw \int_0^\infty dr' \int_{-\infty}^\infty dw' \\
&\quad \tilde{\rho}_B(r,w)\tilde{K}^{-1}(r,w;r',w')\tilde{\rho}_B(r',w'), \qquad \text{(B2)}
\end{aligned}
$$

using $\tilde{\rho}_B(r,w) \equiv r^2\rho_B(r,w)$ and the hermite kernel $\tilde{K} \equiv 4\pi r^2 K$ in (r,w)-space.

On the lattice, the kernel $\tilde{K}$ in Eq. (29) is transformed into a differential form and is expressed as a matrix $\tilde{K}_L(r,w;r',w')$. Then, the kernel inverse $\tilde{K}_L^{-1}(r,w;r',w')$ is numerically obtained by taking the inverse matrix of the kernel $\tilde{K}_L(r,w;r',w')$. As a technical caution, the kernel $\tilde{K}_L(r,w;r',w')$ has a translational zero mode, reflecting the derivative form of $\tilde{K}$. Since this translational zero mode does not affect the total energy, the inverse of $\tilde{K}$ has to be taken in the space except the spurious zero mode. In fact, using an orthogonal matrix O, the kernel $\tilde{K}_L$ is diagonalized as

$$
\tilde{K}_L = O\,\mathrm{diag}(0,\lambda_1,\lambda_2,\cdots)O^T \qquad \text{(B3)}
$$

with nonzero eigenvalues λ_n. Then, we define its inverse $\tilde{K}_L^{-1}$ to be

$$
\tilde{K}_L^{-1} = O\,\mathrm{diag}(0,\lambda_1^{-1},\lambda_2^{-1},\cdots)O^T, \qquad \text{(B4)}
$$

which is equivalent to the appropriate removal of the spurious translational zero mode. Using this kernel inverse $\tilde{K}_L^{-1}$ and the baryon density ρ_B, the energy $E^{\mathrm{U}(1)}$ of the CS term is calculated as $\rho_B\tilde{K}_L^{-1}\rho_B$ on the lattice.

Thus, for the numerical calculation of $E_{\mathrm{U}(1)}$, there are two different methods: one is to update the holographic fields $\phi(r,w)$, $\vec{a}(r,w)$ and $\hat{A}_0(r,w)$ on the lattice based on Eq. (28); the other is to update only $\phi(r,w)$ and $\vec{a}(r,w)$ using Eq. (B2). We have confirmed that both methods give the same numerical results for holographic baryons.

APPENDIX C: HOLOGRAPHIC BARYON USING SELF-DUAL BPS INSTANTON

In Appendix C, we investigate the holographic baryon when the self-dual BPS instanton in Eq. (56) is used. The self-dual BPS instanton is the 't Hooft solution of the ordinary Yang-Mills theory, and hence, to be strict, this usage is justified in the case of flat space $h(w) = k(w) = 1$ and ignoring the CS term. Substituting the BPS instanton with the size R into the total energy E in Eq. (30) including the CS term and the background gravity, $k(w) = 1 + w^2$ and $h(w) = k(w)^{-1/3}$, one obtains the static baryon energy $E(R) = V^{\mathrm{BPS}}(R)$ as the function of the instanton size R, and its minimum gives an approximate ground-state holographic baryon, which satisfies $M_B^{\mathrm{BPS}} \simeq 1.35\ M_{\mathrm{KK}} \simeq 1.28$ GeV and $\sqrt{\langle r^2 \rangle_{\rho_B}^{\mathrm{BPS}}} = \sqrt{\frac{3}{2}} R_0^{\mathrm{BPS}} \simeq 2.2\ M_{\mathrm{KK}}^{-1} \simeq 0.46$ fm, as shown in Fig. 14. Thus, when the self-dual BPS instanton is used, the holographic ground-state baryon has larger mass and smaller size [19] than the true solution numerically obtained in Sec. IV.

For the approximate ground-state holographic baryon, the corresponding Higgs field ϕ and gauge field $\vec{a}$ are shown in Fig. 11. These fields give a topological density ρ_B, and $\hat{A}_0$ is obtained by solving EOM (25), as shown in Fig. 12. Figure 13 shows the r^2-multiplied topological and the energy densities.

The static baryon energy $V^{\mathrm{BPS}}(R)$ for the BPS configuration is shown in Fig. 14, and it is approximately fit with a quadratic function,

$$V^{\mathrm{BPS}}(R) \simeq A^{\mathrm{BPS}}(R - R_0^{\mathrm{BPS}})^2 + M^{\mathrm{BPS}},$$
$$A^{\mathrm{BPS}} \simeq 0.39, \qquad R_0^{\mathrm{BPS}} \simeq 1.8, \qquad M_0^{\mathrm{BPS}} \simeq 1.4, \quad \text{(C1)}$$

in the $M_{\mathrm{KK}} = 1$ unit.

Thus, when the self-dual BPS instanton is used, the holographic baryon has larger mass and smaller size [19] than the true solution numerically obtained in Sec. IV.

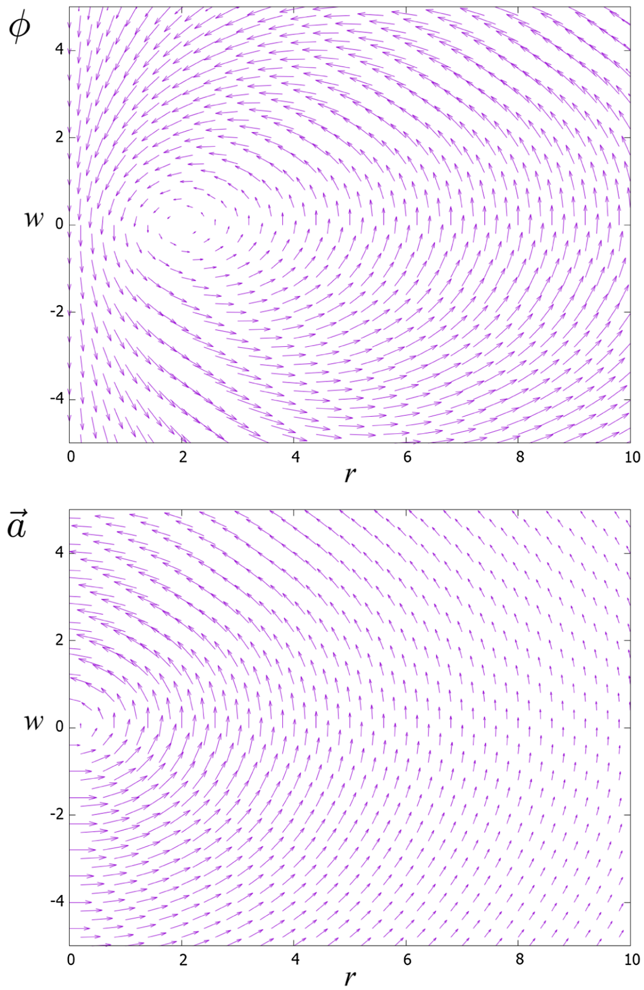

FIG. 11. The Higgs field $\phi(r, w)$ (upper) and the Abelian gauge field $a(r, w) = (a_1, a_2)$ (lower) for the BPS instanton in the Landau gauge in the $M_{\mathrm{KK}} = 1$ unit. For iterative improvement in the main sections, this configuration is used as the starting point, i.e., the initial configuration of the iteration.

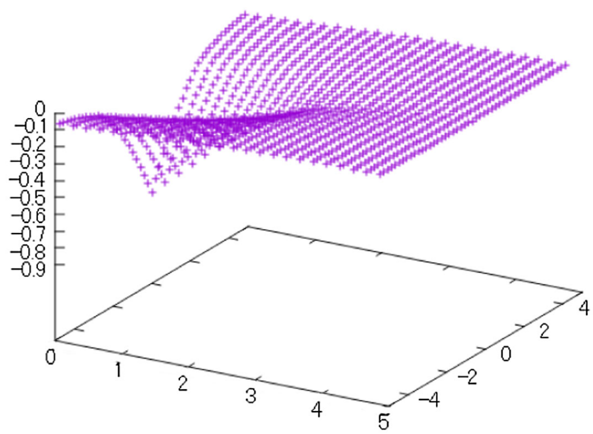

FIG. 12. The U(1) gauge field $\hat{A}_0$ in the case of BPS instanton in the $M_{\mathrm{KK}} = 1$ unit. This is obtained by solving Eq. (25) for the self-dual 't Hooft instanton.

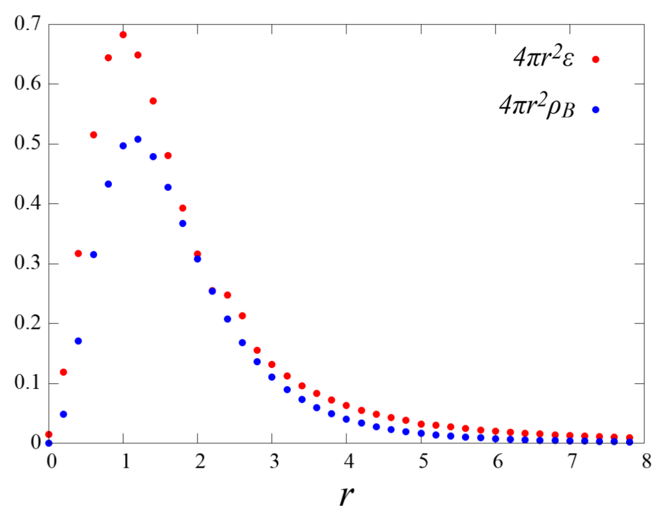

FIG. 13. r^2-multiplied topological and energy densities, $4\pi r^2 \rho_B(r)$ and $4\pi r^2 \mathcal{E}(r)$, in the case of the BPS instanton configuration in the $M_{\mathrm{KK}} = 1$ unit.

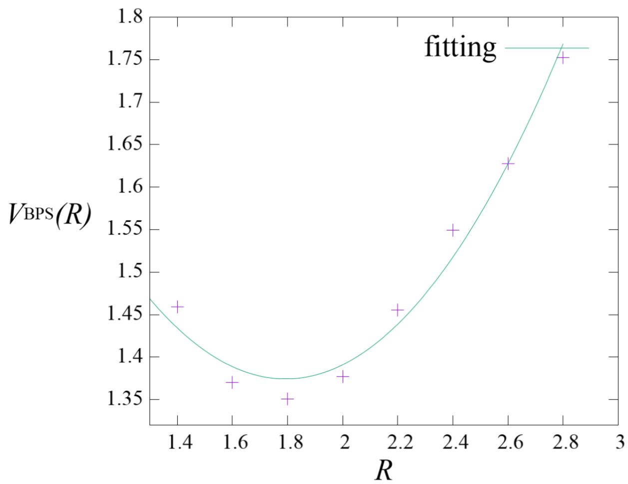

FIG. 14. Static baryon energy $V^{\mathrm{BPS}}(R)$ calculated from the BPS configurations in Eq. (56). The solid line is a fitting curve of quadratic function.

APPENDIX D: ROUGH ANALYTICAL ESTIMATION FOR DILATION MODES USING SELF-DUAL BPS INSTANTON

In Appendix D, we consider a rough analytical estimation of the dilation mode using the self-dual 't Hooft BPS instanton, which is justified in the flat space $h(w) = k(w) = 1$ and without the CS term.

In this case, when the flat space approximation $h(w) = k(w) = 1$ is used, the kinetic term T of the size variable $R(t)$ is analytically expressed as

$$\begin{aligned} T &\simeq \kappa \int d^3x\, dw\, \mathrm{tr}[F_{0M}^2] \\ &\simeq \kappa \int d^3x\, dw \frac{24x^2}{(x^2+R_0^2)^4} R_0^2 \dot{R}^2 \\ &= 48\pi^2\kappa \int dr \frac{r^5}{(r^2+R_0^2)^4} R_0^2 \dot{R}^2 \\ &= 8\pi^2\kappa \dot{R}^2 = \frac{1}{2} m_R \dot{R}^2, \end{aligned} \tag{D1}$$

where $\dot{R}$ means $\partial_t R$. Here, $h(w) = k(w) = 1$ is used in the first line, and the instanton size R_0 appearing in the middle does not affect the result. In this way, the mass parameter m_R on the size variation is estimated as

$$m_R = 16\pi^2\kappa \simeq 1.18. \tag{D2}$$

Form this mass parameter m_R and the potential $V^{\mathrm{BPS}}(R)$ in Eq. (C1), one obtains a rough estimation of the excitation energy of the dilatation mode,

$$\omega = \sqrt{\frac{2A^{\mathrm{BPS}}}{m_R}} = 0.81\ M_{\mathrm{KK}} \simeq 771\ \mathrm{MeV}, \tag{D3}$$

which seems a larger value than the numerical result in Sec. VI. This estimation can be analytically done but has no gravitational effect of $h(w)$ and $k(w)$ for both kinetic and potential terms, in addition to use of the self-dual BPS instanton. On these points, the numerical calculation presented in Sec. VI has been developed.

[1] J. M. Maldacena, The large N limit of superconformal field theories and supergravity, Adv. Theor. Math. Phys. **2**, 231 (1998).
[2] J. Polchinski, Dirichlet branes and Ramond-Ramond charges, Phys. Rev. Lett. **75**, 4724 (1995); *String Theory*, Cambridge Monographs on Mathematical Physics (Cambridge University Press, Cambridge, England, 1998).
[3] E. Witten, Anti-de Sitter space and holography, Adv. Theor. Math. Phys. **2**, 253 (1998); Anti-de Sitter space, thermal phase transition, and confinement in gauge theories, Adv. Theor. Math. Phys. **2**, 505 (1998).
[4] M. Kruczenski, D. Mateos, R. C. Myers, and D. J. Winters, Towards a holographic dual of large-N_c QCD, J. High Energy Phys. 05 (2004) 041.
[5] T. Sakai and S. Sugimoto, Low energy hadron physics in holographic QCD, Prog. Theor. Phys. **113**, 843 (2005); More on a holographic dual of QCD, Prog. Theor. Phys. **114**, 1083 (2005).
[6] Y. Nambu, *Duality and hadrodynamics, Notes prepared for the Copenhagen High Energy Symposium* (1970) (unpublished).
[7] T. Goto, Relativistic quantum mechanics of one-dimensional mechanical continuum and subsidiary condition of dual resonance model, Prog. Theor. Phys. **46**, 1560 (1971).
[8] A. M. Polyakov, Quantum geometry of bosonic strings, Phys. Lett. **103B**, 207 (1981).
[9] M. B. Green, J. Schwarz, and E. Witten, *Superstring Theory* (Cambridge University Press, Cambridge, England, 1987), and its references.
[10] A. Karch and E. Katz, Adding flavor to AdS/CFT, J. High Energy Phys. 06 (2002) 043.
[11] J. Erlich, E. Katz, D. Son, and M. Stephanov, QCD and a holographic model of hadrons, Phys. Rev. Lett. **95**, 261602 (2005).
[12] E. Witten E, Baryons in the 1/N expansion, Nucl. Phys. **B160**, 57 (1979).

[13] T. H. R. Skyrme, A nonlinear field theory, Proc. R. Soc. A **260**, 127 (1961); A unified field theory of mesons and baryons, Nucl. Phys. **31**, 556 (1962).
[14] I. Zahed and G. E. Brown, The Skyrme model, Phys. Rep. **142**, 1 (1996).
[15] M. Gell-Mann, A schematic model of baryons and mesons, Phys. Lett. **8**, 214 (1964); G. Zweig, Report No. CERN-TH-401, CERN-TH-412 (1964) (unpublished).
[16] K. Nawa, H. Suganuma, and T. Kojo, Baryons in holographic QCD, Phys. Rev. D **75**, 086003 (2007).
[17] K. Nawa, H. Suganuma, and T. Kojo, Brane-induced Skyrmion on S^3: Baryonic matter in holographic QCD, Phys. Rev. D **79**, 026005 (2009).
[18] E. Witten, Baryons and branes in anti-de Sitter space, J. High Energy Phys. 07 (**1998**) 006.
[19] H. Hata, T. Sakai, S. Sugimoto, and S. Yamato, Baryons from instantons in holographic QCD, Prog. Theor. Phys. **117**, 1157 (2007).
[20] K. Hashimoto, T. Sakai, and S. Sugimoto, Holographic baryons: Static properties and form factors from gauge/string duality, Prog. Theor. Phys. **120**, 1093 (2008).
[21] D. K. Hong, M. Rho, H. U. Yee, and P. Yi, Chiral dynamics of baryons from string theory, Phys. Rev. D **76**, 061901 (2007); Dynamics of baryons from string theory and vector dominance, J. High Energy Phys. 09 (2007) 063.
[22] A. Cherman and T. Ishii, Long-distance properties of baryons in the Sakai-Sugimoto model, Phys. Rev. D **86**, 045011 (2012).
[23] S. Bolognesi and P. Sutcliffe, The Sakai-Sugimoto soliton, J. High Energy Phys. 01 (2014) 078.
[24] M. Rozali, J. B. Stang, and M. van Raamsdonk, Holographic baryons from oblate instantons, J. High Energy Phys. 02 (2014) 044.
[25] L. D. Roper, Evidence for a P_{11} pion-nucleon resonance at 556 MeV, Phys. Rev. Lett. **12**, 340 (1964).
[26] C. Hajduk and B. Schwesinger, The breathing mode of nucleons and Δ-isobars in the Skyrme model, Phys. Lett. **140B**, 172 (1984).
[27] A. Hayashi and G. Holzwarth, Excited nucleon states in the Skyrme model, Phys. Lett. **140B**, 175 (1984).
[28] I. Zahed, U.-G. Meissner, and U. B. Kaulfuss, Low-lying resonances in the Skyrme model using the semi-classical approximation, Nucl. Phys. **A426**, 524 (1984).
[29] H. Walliser and G. Eckart, Baryon resonance as fluctuations of the Skyrme soliton, Nucl. Phys. **A429**, 514 (1984).
[30] K. F. Liu, J. S. Zhang, and G. R. E. Black, Time dependence of the Skyrme soliton, Phys. Rev. D **30**, 2015 (1984).
[31] J. Breit and C. R. Nappi, Phase shifts of the Skyrmion breathing mode, Phys. Rev. Lett. **53**, 889 (1984).
[32] N. Mathur, Y. Chen, S. J. Dong, T. Draper, I. Horváth, F. X. Lee, K. F. Liu, and J. B. Zhang, Roper resonance and $S_{11}(1535)$ from lattice QCD, Phys. Lett. B **605**, 137 (2005).
[33] B. G. Lasscock, J. N. Hedditch, W. Kamleh, D. B. Leinweber, W. Melnitchouk, A. G. Williams, and J. M. Zanotti, Even parity excitations of the nucleon in lattice QCD, Phys. Rev. D **76**, 054510 (2007).
[34] H. Suganuma and K. Hori, Topological objects in holographic QCD, Phys. Scr. **95**, 074014 (2020).
[35] A. A. Belavin, A. M. Polyakov, A. S. Schwartz, and Yu. S. Tyupkin, Pseudoparticle solutions of the Yang-Mills equations, Phys. Lett. **59B**, 85 (1975).
[36] G.'t Hooft, Computation of the quantum effects due to a four-dimensional pseudoparticle, Phys. Rev. D **14**, 3432 (1976).
[37] E. Witten, Some exact multi-instanton solutions of classical Yang-Mills theory, Phys. Rev. Lett. **38**, 121 (1977).
[38] K. Hashimoto, T. Sakai, and S. Sugimoto, Nuclear force from string theory, Prog. Theor. Phys. **122**, 427 (2009).
[39] M. Gell-Mann, R. J. Oakes, and B. Renner, Behavior of current divergences under $\mathrm{SU}(3) \times \mathrm{SU}(3)$, Phys. Rev. **175**, 2195 (1968).
[40] R. L. Workman *et al.* (Particle Data Group), Review of particle physics, Prog. Theor. Exp. Phys. **2022**, 083C01 (2022).
[41] G. Adkins, C. R. Nappi, and E. Witten, Static properties of nucleons in the Skyrme model, Nucl. Phys. **B228**, 552 (1983).
[42] K. Matsumoto and H. Suganuma, A Study of the H-dibaryon in Holographic QCD, J. Phys. Soc. Jpn. Conf. Proc. **13**, 020014 (2017); Holographic QCD for H-dibaryon (uuddss), EPJ Web Conf. **137**, 13018 (2017).